bioRxiv preprint doi: https://doi.org/10.1101/499871; this version posted December 19, 2018. The copyright holder for this preprint (which was not certified by peer review) is the author/funder, who has granted bioRxiv a license to display the preprint in perpetuity. It is made available under aCC-BY 4.0 International license.

Original Research

Immunomodulatory activity of *Ganoderma lucidum* immunomodulatory protein *via* PI3K/Akt and MAPK signaling pathways in macrophage RAW264.7 cells

Qi-Zhang Li,[a,b] Yu-Zhou Chang,[c] Liu-Ding-Ji Li,[b] Xiao-Yu Du,[b] Xiao-Hui Bai,[b] Zhu-Mei He,[a*] Lei Chen,[c*] Xuan-Wei Zhou,[b*]

[a]Guangdong Provincial Key Laboratory for Aquatic Economic Animals, School of Life Sciences, Sun Yat-sen University, Guangzhou, People's Republic of China

[b]School of Agriculture and Biology, and Engineering Research Center of Therapeutic Antibody (Ministry of Education), Shanghai Jiao Tong University, Shanghai, People's Republic of China

[c]Center for Microbiota and Immunological Diseases, Shanghai General Hospital, Shanghai Institute of Immunology, School of Medicine, Shanghai Jiao Tong University, Shanghai, People's Republic of China

Running title: Immunomodulatory activity of *G. lucidum* FIP

---

*Corresponding authors: Prof. Xuan-Wei Zhou, No. 1-411# Agriculture and Biology Building, 800 Dongchuan Road, Shanghai Jiao Tong University, Shanghai 200240, People's Republic of China. Tel. & Fax.: +86-21-34205778, E-mail: xuanweizhou@sjtu.edu.cn; Prof. Lei Chen, E-mail: lei.chen@sjtu.edu.cn. Prof. Zhu-Mei He, School of Life Sciences, Sun Yat-sen University, Guangzhou, People's Republic of China. Tel. & Fax.: +86-020-84113065, E-mail: lsshezm@mail.sysu.edu.cn.

bioRxiv preprint doi: https://doi.org/10.1101/499871; this version posted December 19, 2018. The copyright holder for this preprint (which was not certified by peer review) is the author/funder, who has granted bioRxiv a license to display the preprint in perpetuity. It is made available under aCC-BY 4.0 International license.

ABSTRACT

Ganoderma lucidum, a traditional edible and medicinal fungus, holds an important status in health care systems in China and other Asian countries. Fungal immunomodulatory protein (FIP), one of the active ingredients isolated from *G. lucidum*, is a class of naturally occurring proteins and possesses potential biological functions. This study was conducted to explore the molecular mechanism of its immunomodulatory potency in immune responses of macrophages. *In vitro* assays of biological activity indicated that rFIP-glu significantly activated macrophage RAW264.7 cells, and possessed the ability of pro- and anti-inflammation the cells. RNA sequencing analysis showed that macrophage activation involved Toll-like receptors and mitogen-activated protein kinases pathways. Furthermore, qRT-PCR indicated that phosphoinositide 3 kinase inhibitor LY294002 blocked the mRNA levels of MCP-1, MEK1/2 inhibitor U0126 reduced the mRNA levels of TNF-α and MCP-1, and JNK inhibitor SP600125 prevented the up-regulation of iNOS mRNA in the rFIP-glu-induced cells. FIP-glu mediated these inflammatory effects not through a general pathway, instead through a different pathway for different inflammatory mediator. These data indicate the possibility that rFIP-glu has an important immune-regulation function and thus has potential therapeutic uses.

KEYWORDS

Ganoderma lucidum immunomodulatory protein (FIP-glu); immunomodulatory; RNA sequencing (RNA-seq); mitogen-activated protein kinases (MAPK); phosphoinositide 3 kinase (PI3K)

bioRxiv preprint doi: https://doi.org/10.1101/499871; this version posted December 19, 2018. The copyright holder for this preprint (which was not certified by peer review) is the author/funder, who has granted bioRxiv a license to display the preprint in perpetuity. It is made available under aCC-BY 4.0 International license.

Ganoderma lucidum, a traditional Chinese medicinal mushroom, is a species in the genus of *Ganoderma* with numerous pharmacological effects such as improving immune function, antitumor, antioxidant, reducing cardiovascular and cerebrovascular diseases and heart diseases caused by body oxidation (1). Among more than 400 different bioactive compounds isolated from *G. lucidum*, fungal immunomodulatory protein (FIP) is an important bioactive component with immune regulating activity and is one of the most promising active ingredients developed by modern biotechnologies (2). FIP is a small protein with similar structure and immune-regulatory activity to phytohemagglutinin and immunoglobulins. Since the first FIP (designated as Lingzhi-8 or LZ-8) was isolated from *G. lucidum* mycelia, dozens of FIPs have been isolated and identified from different fungous species in recent years (3-6). FIPs have immunomodulatory functions and play an important role in anti-tumor, anti-allergy, anti-transplant rejection, *etc*., which implies a promising application for medicinal use (7). For example, FIPs suppress tumors by inhibition of telomerase activity *via* decrease of *hTERT* promoter activity and translocation of its protein (8-10). FIP-gmi induce apoptosis *via* β-catenin inhibition in lung cancer cells (11). FIP-fve has anti-inflammatory effects on OVA-induced airway inflammation and reduces airway remodeling by suppressing IL-17 (12). In spite of a few studies about anti-tumor (13, 14) and immunomodulatory effects (15-17), the mechanism of these activities remain unclear. The relationship between the activation of these proteins, downstream cytokine expression and physiological function represents an active line of investigation.

bioRxiv preprint doi: https://doi.org/10.1101/499871; this version posted December 19, 2018. The copyright holder for this preprint (which was not certified by peer review) is the author/funder, who has granted bioRxiv a license to display the preprint in perpetuity. It is made available under aCC-BY 4.0 International license.

Macrophages, belonging to a group of mononuclear phagocytes, play vital roles in processes of the immune response and are strategically positioned throughout the body tissues (18). They possess functions of phagocytosis, antigen presentation and production of cytokines, thereby initiating immune response (19). Following activation, macrophages can release a wide array of pro- or anti-inflammatory cytokines, which further activate fellow immune cells (20). Depending on these signals, macrophages have been typed classically activated (pro-inflammation, M1) and alternatively activated (anti-inflammation, M2) (21). Classically activated macrophages are elicited in response to pro-inflammatory cytokines and pathogen-associated molecular patterns (PAMPs), such as Interferon-γ (IFN-γ) and lipopolysaccharide (LPS) to promote pathogen killing and chronic inflammation. (22, 23). These macrophages produce cytotoxic and inflammatory molecules nitric oxide (NO) and reactive oxygen species (ROS), pro-inflammatory cytokines tumor necrosis factor (TNF-α), interleukin (IL)-1β and IL-6, chemokine monocyte chemoattractant protein-1 (MCP-1, or C-C motif ligand 2 (CCL-2)), *etc*. (24). However, excessive inflammatory mediators can be implicated in a number of chronic diseases, such as arthritis, colitis and asthma (25). M2 macrophages, which are typed in response to anti-inflammatory cytokines, parasitic infections and damage-associated molecular patterns (DAMPs), such as IL-4 and IL-13, play an important role in inhibition of chronic and acute inflammatory response and in tissue repair (23). M2 macrophages are able to secrete high amounts of anti-inflammatory cytokines, such as IL-10 and TGF-β (26).

bioRxiv preprint doi: https://doi.org/10.1101/499871; this version posted December 19, 2018. The copyright holder for this preprint (which was not certified by peer review) is the author/funder, who has granted bioRxiv a license to display the preprint in perpetuity. It is made available under aCC-BY 4.0 International license.

92 Macrophages can be activated to an inflammation-promoting phenotype through
93 members of the Toll-like receptor (TLR) family such as TLR4 (20, 27, 28). Activated
94 TLRs induce activation of specific intracellular pathways including phosphoinositide
95 3 kinases (PI3K/Akt), mitogen activated protein kinases (MAPKs) and nuclear factor
96 kappa B (NF-κB) (21, 29, 30). PI3K/Akt signaling pathway participates in
97 macrophage polarization (31-34), while MAPKs, including extracellular
98 signal-related kinase (ERK)-1/2, p38 and c-Jun NH2-terminal kinase (JNK), and
99 NF-κB are classic inflammation related signals and induce the expression of
100 pro-inflammatory mediators (35-38).
101 Here, we report that rFIP-glu produced in *Pichia pastoris* has the ability to induce
102 macrophage activation and produce pro- and anti-inflammatory mediators, which may
103 be through PI3K and MAPK pathways.
104

105 ## RESULTS

106 **Production of rFIP-glu in *Pichia pastoris*.** An expression vector pPIC9K
107 was used for achieving rFIP-glu. To facilitate purification, a His-tag was added at the
108 C-terminal of rFIP-glu (Fig. 1A). Following confirmation by sequencing and
109 linearization by *Sac I*, a recombination plasmid containing nucleotide sequences of
110 FIP-glu and His-tag was transformed into *Pichia pastoris* GS115 cells. The
111 transformants successfully secreted recombination proteins into the media compared
112 with the negative control (GS115 transformed with or without pPIC9K plasmid
113 incubated with or without MeOH) after induced by MeOH for 72 h (Fig. 1B). Western

bioRxiv preprint doi: https://doi.org/10.1101/499871; this version posted December 19, 2018. The copyright holder for this preprint (which was not certified by peer review) is the author/funder, who has granted bioRxiv a license to display the preprint in perpetuity. It is made available under aCC-BY 4.0 International license.

114 blot analysis further confirmed that the secreted protein was rFIP-glu using anti-6×His
115 tag (Fig. 1C) and anti-rFIP-glu (Fig. 1D).
116
117 **Toxicity of rFIP-glu against RAW264.7 cells.** To investigate the activation
118 effect of rFIP-glu on the RAW264.7 cells, firstly we determined whether this
119 recombinant fungal protein possessed toxicity and measured its noncytotoxic range.
120 As shown in Fig. 2, the proliferation of RAW265.7 cells treated with 1 and 2 μg/mL
121 of rFIP-glu significantly increased ($p \leq 0.0001$), relative to the control group. A
122 culture of RAW264.7 cells incubated with 4 μg/mL of rFIP-glu resulted in no effect
123 on cell viability and more than 90% of cells with 8 μg/mL were viable ($p \leq 0.01$). The
124 viability of RAW264.7 cells with more than 8 μg/mL showed a rapid decease ($p \leq$
125 0.0001). Based on these results, subsequent assays were performed at 4 μg/mL or no
126 more than 8 μg/mL. Additionally, rFIP-glu obviously influenced the morphology of
127 RAW264.7 macrophages with or without stimulation of LPS (Fig. S1).
128
129 **rFIP-glu improves phagocytosis of RAW264.7 cells.** Next, phagocytic
130 activities of RAW264.7 cells treated with rFIP-glu were examined by neutral red
131 uptake assay. As shown in Fig. 3, when the cells were treated with noncytotoxic
132 concentration of rFIP-glu ranged from 1 to 8 μg/mL, the phagocytosis increased and
133 then decreased. The phagocytosis of macrophage RAW264.7 cells were significantly
134 improved ($p \leq 0.05$) at 2 μg/mL of rFIP-glu, but suppressed ($p > 0.05$) at 8 μg/mL.
135 These indicate that rFIP-glu has the ability to enhance phagocytic activity of RAW

bioRxiv preprint doi: https://doi.org/10.1101/499871; this version posted December 19, 2018. The copyright holder for this preprint (which was not certified by peer review) is the author/funder, who has granted bioRxiv a license to display the preprint in perpetuity. It is made available under aCC-BY 4.0 International license.

264.7 cells when the concentration is no higher than 8 μg/mL.

rFIP-glu regulates pro- and anti-inflammatory genes at transcriptional level in RAW264.7 cells. To further evaluate the immunostimulatory effects of rFIP-glu, we investigated whether rFIP-glu had the ability to induce mRNA levels of relevant genes contributing to the function of macrophages. These genes were determined by qRT-PCR after cells were treated with rFIP-glu (1, 2, 4 and 8 μg/mL) for 6 h (Fig. 4). Compared to control, the rFIP-glu-treated group showed a robust increase in the mRNA level of TNF-α (Fig. 4A; $p \leq 0.01$ at 1 μg/mL; $p \leq 0.001$ at 2, 4 and 8 μg/mL). Similarly, rFIP-glu also significantly promoted the mRNA expression of Arginase II in a concentration-dependent manner (Fig. 4B; $p \leq 0.001$ at 1 μg/mL; $p \leq 0.0001$ at 2, 4 and 8 μg/mL). The production of NO was measured firstly, but none was detected at 1 to 8 μg/mL of rFIP-glu (Data not shown). Alternatively, we investigated the mRNA expression of iNOS and found that it also dramatically increased in a concentration-dependent manner (Fig. 4C; $p \leq 0.0001$ at 4 and 8 μg/mL). The mRNA level of MCP-1 (CCL-2) was also increased and peaked at 2 μg/mL ($p \leq 0.0001$), and then decreased to no change at 8 μg/mL compared with control (Fig. 4D). rFIP-glu treatment concentration-dependently inhibited the mRNA expression levels of IL-10 (Fig. 4E; $p \leq 0.0001$) in RAW264.7 cells. These results exhibit that rFIP-glu stimulates the immune responses by inducing pro-inflammatory mediators. In parallel, rFIP-glu inhibited the mRNA expression level of CXCL-10 (Fig. 4F; $p \leq 0.01$ at 1

bioRxiv preprint doi: https://doi.org/10.1101/499871; this version posted December 19, 2018. The copyright holder for this preprint (which was not certified by peer review) is the author/funder, who has granted bioRxiv a license to display the preprint in perpetuity. It is made available under aCC-BY 4.0 International license.

158 μg/mL; $p \leq 0.0001$ at 2, 4 and 8 μg/mL). This result exhibits that rFIP-glu induces
159 anti-inflammatory phenotype of macrophages. Additionally, there was little or no
160 effect on IL-6 at transcriptional level (Fig. 4G) and the mRNA expression of IL-1β
161 was not detected (Data not shown). Taken together, rFIP-glu re-polarizes
162 macrophages by regulating of pro- and anti-inflammatory genes expression at
163 transcriptional level in RAW264.7 cells.
164
165 **rFIP-glu regulates LPS-induced pro- and anti-inflammatory**
166 **mediators at transcriptional level in RAW264.7 cells.** In order to further
167 determine that rFIP-glu induces or suppresses mRNA expression levels of pro- and
168 anti-inflammatory genes, RAW264.7 cells were stimulated with 1 μg/mL LPS in the
169 presence or absence of increasing concentration of rFIP-glu for 6 h, and then
170 qRT-PCR analysis was performed. Compared with the normal control group, LPS
171 treatment (1 μg/mL) significantly increased the mRNA expression of IL-1β, IL-6,
172 IL-10, TNF-α, MCP-1 (CCL-2), CXCL-10 and Arginase II and production of NO (Fig.
173 5). rFIP-glu treatment (1, 2, 4 and 8 μg/mL) significantly promoted the mRNA levels
174 of TNF-α (Fig. 5A; $p \leq 0.0001$), MCP-1 (CCL-2) (Fig. 5B; $p \leq 0.0001$) and Arginase
175 II (Fig. 5C; $p \leq 0.0001$) and concentration-dependently inhibited IL-10 expression at
176 transcriptional level (Fig. 5D; $p \leq 0.001$ at 2 μg/mL; $p \leq 0.0001$ at 4 and 8 μg/mL) in
177 LPS-stimulated RAW 264.7 cells. These results suggest that rFIP-glu promotes
178 inflammation in LPS-induced RAW264.7. On the other hand, rFIP-glu could
179 suppressed LPS-induced mRNA expression levels of IL-1β (Fig. 5E; $p \leq 0.01$ at 2

bioRxiv preprint doi: https://doi.org/10.1101/499871; this version posted December 19, 2018. The copyright holder for this preprint (which was not certified by peer review) is the author/funder, who has granted bioRxiv a license to display the preprint in perpetuity. It is made available under aCC-BY 4.0 International license.

μg/mL; $p \leq 0.0001$ at 4 and 8 μg/mL), IL-6 (Fig. 5F; $p \leq 0.01$ at 4 μg/mL; $p \leq 0.0001$ at 8 μg/mL) and CXCL-10 (Fig. 5G; $p \leq 0.01$ at 4 μg/mL; $p \leq 0.0001$ at 8 μg/mL) and LPS-induced production of NO (Fig. 5H; $p \leq 0.01$ at 2 μg/mL; $p \leq 0.0001$ at 4 and 8 μg/mL) in a concentration-dependent manner. The results indicate that rFIP-glu suppresses the LPS-induced expression of these inflammatory mediators at the transcriptional level. Thus, rFIP-glu regulates pro- and anti-inflammatory genes expression at transcriptional level in LPS-stimulated RAW264.7 cells.

RNA sequencing results. To give further insights into the molecular mechanisms involved in the activity of rFIP-glu on macrophage RAW264.7 cells, RNA-seq was performed at the sequencing core facility of Shanghai Institute of Immunology. RAW264.7 cells were exposed to non-toxic rFIP-glu doses (4 μg/mL) for 6 h (Fig. 6). There were approximately 50,000 (coding and non-coding) genes detected. To determine sample relationships, principle component analysis (PCA) (Fig. 6A) and hierarchical clustering analysis (Heatmap) (Fig. 6B) were performed and demonstrated that two different groups, rFIP-glu treatment group and control (PBS) group, can be distinguished and showed segregation. Using an FDR ≤ 0.001 and fold change > 1 to determine differently expressed genes after rFIP-glu treatment, more than 700 genes were differentially expressed and we observed 578 up-regulated genes and 159 down-regulated gene (Fig. 6C). Next, we used the Gene Ontology (GO) database to characterize the differentially expressed genes. Subsets of these genes were found to be involved in cellular process, regulation of biological process,

bioRxiv preprint doi: https://doi.org/10.1101/499871; this version posted December 19, 2018. The copyright holder for this preprint (which was not certified by peer review) is the author/funder, who has granted bioRxiv a license to display the preprint in perpetuity. It is made available under aCC-BY 4.0 International license.

metabolic process, response to stimulus, developmental process, signaling and localization (Fig. 6D). These genes encoded proteins that perform immunological functions including inflammatory response, response to oxygen-containing compound, cellular response to organonitrogen compound, regulation of protein phosphorylation, regulation of protein modification process and regulation of programmed cell death (Fig. 6E). Moreover, to investigate the possible signaling pathways through which RAW264.7 cells activated by rFIP-glu, Kyoto Encyclopedia of Genes and Genomes (KEGG) pathway enrichment analysis was performed. Fig. 6F showed the top 20 significantly enriched canonical pathways. In order to verify the RNA-seq results, 10 differential expression genes which were up- or down-regulated showed in the RNA-seq results were selected. The expression levels of these genes measured by RT-qPCR showed the same tendency with RNA-seq (Fig. 6G).

PI3K and MAPK signaling pathways are involved in rFIP-glu-induced macrophage activation. Obviously, results mentioned above had been shown that rFIP-glu was capable to promote macrophage proliferation and phagocytosis and induce the mRNA expression of inflammatory mediators such as TNF-α, MCP-1 (CCL-2) and iNOS. Analysis of RNA-seq indicated that Toll-like receptors pathway was involved in macrophage activation by rFIP-glu (Fig. S2). Signaling pathway inhibitor, PI3K inhibitor LY294002, was used to further confirm the mechanisms involved in rFIP-glu-induced macrophage activation. mRNA levels of TNF-α, MCP-1 (CCL-2) and iNOS were measure by qRT-PCR. Results showed that PI3K inhibitor

bioRxiv preprint doi: https://doi.org/10.1101/499871; this version posted December 19, 2018. The copyright holder for this preprint (which was not certified by peer review) is the author/funder, who has granted bioRxiv a license to display the preprint in perpetuity. It is made available under aCC-BY 4.0 International license.

LY294002 blocked the mRNA levels of MCP-1 (CCL-2) induced by rFIP-glu in RAW264.7 cells (Fig. 7B; $p \leq 0.0001$), while the mRNA expression of TNF-α was not changed (Fig. 7A). These findings suggest that the PI3K pathway is related to rFIP-glu-induced macrophage activation.

RNA-seq data implied that MAPK signaling pathway was also involved in macrophage activation by rFIP-glu (Fig. S3). Signaling pathway inhibitors, MEK1/2 inhibitor U0126, JNK inhibitor SP600125 and p38 inhibitor SB203580, were used to further confirm the mechanisms involved in rFIP-glu-induced macrophage activation. mRNA levels of TNF-α, MCP-1 (CCL-2) and iNOS were measure by qRT-PCR. Results showed that, in rFIP-glu-induced RAW264.7, MEK1/2 inhibitor U0126 blocked the mRNA levels of TNF-α (Fig. 7C; $p \leq 0.0001$) and MCP-1 (CCL-2) (Fig. 7D; $p \leq 0.0001$) and JNK inhibitor SP600125 prevented the up-regulation of iNOS mRNA (Fig. 7E; $p \leq 0.001$). These findings suggest that the MEK1/2 and JNK pathways are indeed related to rFIP-glu-induced macrophage activation.

Discussion

G. lucidum is well known as an edible medicinal mushroom for thousands of years in China. FIP-glu or LZ-8 is one of the active ingredients in *G. lucidum*. From beginning of discovery, FIP-glu is named immunomodulatory protein because of a certain degree of homology with the heavy chain variable region of several immunoglobulins (39, 40). FIP-glu possesses a variety of physiological activities, such as anti-anaphylaxis, proliferation stimulation of lymphocytes, anti-tumor and

bioRxiv preprint doi: https://doi.org/10.1101/499871; this version posted December 19, 2018. The copyright holder for this preprint (which was not certified by peer review) is the author/funder, who has granted bioRxiv a license to display the preprint in perpetuity. It is made available under aCC-BY 4.0 International license.

246 immunosuppression (7), suggesting that this protein has great potential in
247 development of immuno-regulated drugs or foods. Our results showed that rFIP-glu is
248 a potent stimulator of macrophage proliferation and activation. rFIP-glu can regulate
249 the mRNA expression of pro- and anti-inflammatory mediators in macrophage
250 RAW264.7 cells in the presence or absence of LPS. rFIP-glu mediates macrophage
251 activation through PI3K and MAPK pathways based on RNA-seq analysis.

252 Macrophages play an important role in host-defense. Macrophages perform
253 phagocytosis against pathogens as the first step, which is used to initiate the innate
254 immune response, and then orchestrate the adaptive response (41). Thus, phagocytosis
255 is a key indicator of evaluating macrophage activation. In the present study, rFIP-glu
256 significantly improved the phagocytosis of macrophage RAW264.7 cells at 2 μg/mL,
257 suggesting that rFIP-glu have abilities to enhance phagocytic activity of RAW 264.7
258 cells. The phagocytosis of macrophages can be enhanced by many bioactive
259 substances, such as polysaccharides (42, 43), peptides (44) and proteins (45, 46),
260 alkaloids (47) and phospholipids (48). Phagocytosis is one of the important innate
261 immune responses. Following RNA-seq analysis showed that rFIP-glu-induced
262 phagocytosis of macrophage RAW264.7 cells involved Fcγ receptor-mediated
263 phagocytosis and most genes involved in this process were up-regulated (Fig. S4).
264 There are two general classes of Fcγ receptors (FcγRs), activating receptors that
265 activate effector functions and inhibitory receptors that inhibit these functions (41). In
266 general, activation and inhibitory FcγRs are co-expressed on the same cell (49). The
267 phagocytosis involves the simultaneous clustering of activating and inhibitory FcγRs

bioRxiv preprint doi: https://doi.org/10.1101/499871; this version posted December 19, 2018. The copyright holder for this preprint (which was not certified by peer review) is the author/funder, who has granted bioRxiv a license to display the preprint in perpetuity. It is made available under aCC-BY 4.0 International license.

and is regulated by the ratio of activating to inhibitory FcγRs (50). Moreover, FcγR-mediated phagocytosis is accompanied by the release of inflammatory mediators, and excessive magnitude of the FcγR response could lead to excessive inflammation (50, 51). RNA-seq analysis exhibited down-regulation of an activating receptor, FcγRI and up-regulation of an inhibitory receptor, FcγRIIb, when RAW264.7 cells were treated with 4 μg/mL of rFIP-glu although the enhancement of phagocytosis was not significant. This suggests that rFIP-glu participates in the regulation of the phagocytosis of macrophages and the release of inflammatory mediators. Additionally, FcγRIIb has ability to suppress allergic responses (52-55). This possibly is one of the mechanisms of rFIP-glu-mediated anti-allergy.

In response to an immune challenge, macrophages become activated and produce cytotoxic and inflammatory mediators, such as NO, ROS, TNF-α and IL-6, that contribute to nonspecific immunity (56). Our results implied that rFIP-glu has the predominant role in transcription of pro-inflammatory genes including TNF-α, MCP-1 (CCL-2), Arginase II and iNOS. Macrophages can be activated by biologically active substances such as polysaccharides and proteins to produce the pro-inflammatory molecules (24, 34, 57, 58). Similarly, most mushroom metabolites also activate macrophages to produce various mediators, such as IL-1β, TNF-α and iNOS (59). PCP, an immunomodulatory protein from *Poria cocos*, can promote TNF-α and IL-1β production in RAW 264.7 cells (60). TNF-α are pro-inflammatory cytokines and play an essential role in the immune response and inflammation (61). MCP-1 (CCL-2) is a member of the CC chemokine family and involved in the

bioRxiv preprint doi: https://doi.org/10.1101/499871; this version posted December 19, 2018. The copyright holder for this preprint (which was not certified by peer review) is the author/funder, who has granted bioRxiv a license to display the preprint in perpetuity. It is made available under aCC-BY 4.0 International license.

290 pathogenesis of multiple forms of inflammatory disorders as a mediator of acute and
291 chronic inflammation (62, 63). Arginase II, one of isoforms of arginase, is
292 up-regulated in M1 macrophages by pro-inflammatory stimuli and promotes
293 pro-inflammatory responses (64, 65). iNOS-dependent nitric oxide from activated
294 macrophages as a cytotoxic mediator can function in many diseases including cancer
295 (66). Interestingly, in rFIP-glu-treated macrophage RAW264.7 cells, the mRNA
296 expression of IL-6 was not changed, and that of IL-1β was not detected due to less
297 transcripts possibly (Data not shown), although IL-1β and IL-6 are important
298 pro-inflammatory cytokines as well. Moreover, the mRNA level of IL-10 was
299 suppressed by rFIP-glu. IL-10 is an anti-inflammation cytokine and is secreted by M2
300 macrophages to suppress the inflammation (26, 67). Studies show that an increase in
301 levels of M1 markers such as IL-1β, MCP-1 (CCL-2), TNF-α and iNOS and a
302 decrease or little change in levels of M2 markers such as IL-10 will drive macrophage
303 M1 activation (68-71). The findings of the present investigation contributed to our
304 understanding that rFIP-glu promotes macrophage M1 polarization and initiates
305 pro-inflammatory responses. Unexpectedly, CXCL-10 were down-regulated at mRNA
306 levels in RAW264.7 cells induced by rFIP-glu. CXCL-10, belonging to the CXC
307 family of chemokines, is involved in systemic inflammation and can mediate the
308 recruitment of inflammatory cells (72, 73). Actually, CXCL-10 are expressed under
309 inflammatory conditions in M1 macrophages (74, 75) and their products are reduced
310 in M2 macrophages (76, 77). It seems that rFIP-glu induces M2 phenotypical
311 macrophages to suppress inflammation. To further confirm anti-inflammatory effects

bioRxiv preprint doi: https://doi.org/10.1101/499871; this version posted December 19, 2018. The copyright holder for this preprint (which was not certified by peer review) is the author/funder, who has granted bioRxiv a license to display the preprint in perpetuity. It is made available under aCC-BY 4.0 International license.

of rFIP-glu, these related genes were detected in LPS-stimulated macrophage RAW264.7 cells. Results showed that rFIP-glu indeed possessed anti-inflammation activity through inhibiting LPS-induced mRNA levels of pro-inflammatory mediators (IL-6, IL-1β and CXCL-10) and the production of NO. A vast majority of bioactive substances can attenuate LPS-induced inflammation by decreasing the mRNA levels of pro-inflammatory mediators and increasing anti-inflammatory mediators. Polysaccharides, SGP-1 and SGP-2 isolated from the rhizomes of *Smilax glabra*, significantly suppressed the release of NO, TNF-α and IL-6 from LPS-induced RAW 264.7 cells (78). A prenylated flavonoid, 10-oxomornigrol F (OMF), can inhibit the LPS-induced production of NO, TNF-α, IL-1β and IL-6 in RAW264.7 cells (79). To our surprise, rFIP-glu acted in strong synergy with LPS to induce the mRNA expression levels of TNF-α, MCP-1 (CCL-2) and Arginase II. Meanwhile, mRNA level of IL-10 was still suppressed by rFIP-glu in LPS stimulated RAW264.7 cells. Another immunomodulatory protein, FIP-apo (APP) from *Auricularia polytricha*, also accounts for synergistic effects with LPS by NO and TNF-α production (80). These results mentioned above suggest that rFIP-glu can balance M1/M2 macrophages by regulating pro- and anti-inflammatory mediators and exhibit immunomodulatory activity. This phenomenon may confer macrophages an ability to quickly switch between M1 or M2 associated functions allowing for appropriate responses to stimuli and tissue environment (81). Re-polarization of macrophages is a key role and a promising therapeutic option in many diseases (26, 82). For example, inflammatory bowel diseases can be ameliorated by switching M1 macrophages to M2 (83, 84).

bioRxiv preprint doi: https://doi.org/10.1101/499871; this version posted December 19, 2018. The copyright holder for this preprint (which was not certified by peer review) is the author/funder, who has granted bioRxiv a license to display the preprint in perpetuity. It is made available under aCC-BY 4.0 International license.

Conversion of M2 to M1 phenotype is a potential therapeutic intervention in anti-tumor (85, 86).

Obviously, rFIP-glu has the ability to activate macrophages. The mechanisms were further investigated. In this study, RNA-seq was used to investigate the mechanisms of macrophage activation in rFIP-glu-treated RAW 264.7 cells. Our results indicated that the macrophage activation induced by rFIP-glu involved Toll-like receptors and MAPKs signaling pathways in macrophage RAW264.7 cells, which is consistent with that PI3K/Akt, the downstream of Toll-like receptor, and MAPK are involved in the activation of macrophages (34, 87-89). TLR4 is critical in immune responses and involved mainly in inflammation responses (90). TLR4 can be recognized and activated by many stimuli such as polysaccharides, and its expression increases, and then activates PI3K/Akt and MAPKs pathways, with introduction of a pool of inflammatory mediators (30, 34, 43, 87, 91). In addition, NF-κB involves in macrophage activation as well (24, 34, 92, 93). Similarly, RNA-seq analysis indicated that NF-κB pathway participated in rFIP-glu-mediated macrophage activation. More evidences should be investigated in the future. Although rFIP-glu activated Toll-like receptors, MAPKs and NF-κB pathways, RNA-seq (Fig. S2) and qRT-PCR (Fig. S5) confirmed that the mRNA expression level of TLR4 did not change. It suggests that the mRNA expression of pro-inflammatory genes induced by rFIP-glu was not through activating the TLR4 signaling pathway. RNA-seq analysis showed that TLR2 mRNA expression increased (Fig. S2), presuming TLR2 was a receptor of rFIP-glu. A preliminary yeast two-hybrid experiment showed that rFIP-glu did not interact with

bioRxiv preprint doi: https://doi.org/10.1101/499871; this version posted December 19, 2018. The copyright holder for this preprint (which was not certified by peer review) is the author/funder, who has granted bioRxiv a license to display the preprint in perpetuity. It is made available under aCC-BY 4.0 International license.

356 an extracellular part of TLR2 (Data not shown), suggesting TLR2 possibly was not a
357 receptor of rFIP-glu as well. It is noteworthy that some active substances can activate
358 all of these pathways (34, 57, 88), while some can only activate one or more (30, 87,
359 94). We next used specific PI3K/Akt and MAPKs pathway inhibitors to clarify
360 whether these signaling pathways were involved in macrophage activation induced by
361 rFIP-glu. Our results implied the involvement of PI3K in rFIP-glu mediated MCP-1
362 (CCL-2) mRNA production, MEK1/2 in TNF-α and MCP-1 (CCL-2), and JNK in
363 iNOS. Although the induction of phosphorylated MAPKs and PI3K/Akt receptors was
364 not evaluated by Western blot, the participation of them was confirmed by RNA-seq
365 as well as inhibition of the effects induced by pretreatment with signaling pathway
366 inhibitors. These results indicate that rFIP-glu may enter cells and act with MEK1/2,
367 JNK or PI3K indirectly or directly, and another hypothesis is that rFIP-glu interacts
368 with TLR2 within cells (Fig. 8). In addition, the synergistic activity of rFIP-glu and
369 LPS implied that rFIP-glu could enhance the expression of downstream mediators that
370 are generated by Toll-like receptors pathway (80). Heme oxygenase-1 (HO-1) is an
371 anti-inflammatory enzyme and attenuates the inflammatory response (95), which can
372 be regulated by nuclear factor erythroid 2-related factor 2 (Nrf2) in the inflammatory
373 response (96). The Induction of HO-1 can be though MAPK and PI3K signaling
374 pathways (94, 97, 98). In the present study, mRNA level of HO-1 was significantly
375 increased in rFIP-glu-induced RAW264.7 cells (Fig. S6). This result implies that the
376 anti-inflammation of rFIP-glu is possibly mediated by HO-1 in macrophage
377 RAW264.7 cells.

bioRxiv preprint doi: https://doi.org/10.1101/499871; this version posted December 19, 2018. The copyright holder for this preprint (which was not certified by peer review) is the author/funder, who has granted bioRxiv a license to display the preprint in perpetuity. It is made available under aCC-BY 4.0 International license.

MATERIALS AND METHODS

Reagents. Neutral red staining solution was obtained from Sangon Biotech (Shanghai, China). U0126 (MEK1/2 inhibitor), SP600125 (JNK inhibitor) and SB203580 (p38 inhibitor) were purchased from Beyotime (Shanghai, China). LY294002 (PI3K inhibitor) was purchased from Selleck Chemicals (Houston, TX, USA). Anti-FIP-glu antiserum was raised in rabbits (99). Anti-6×His Tag mouse monoclonal antibody, HRP-conjugated Goat Anti-Mouse IgG and HRP-conjugated Goat Anti-Rabbit IgG were from Sangon Biotech (Shanghai, China).

Production of rFIP-glu. Production of recombinant FIP-glu (rFIP-glu) in *P. pastoris* was performed according to the instruction provided by Pichia Expression Kit (Invitrogen, USA). Briefly, a gene encoding FIP-glu and subcloned in pUC-57 vector was synthesized by Sangon Biotech (Shanghai) Co., Ltd. (China) based on codon usage bias. Then, the gene was cloned into an expression cassette vector pPIC9K. For convenience, a His-tag was added at 3' end of multiple clone sites of the vector. After construction, the recombinant expression vector pPIC9K-glu-His linearized by a restriction enzyme *Sac* I was transferred into *P. pastoris* GS115. After confirmed by PCR (100) and sequencing, the transformant was induced by methanol for producing rFIP-glu. The rFIP-glu was purified with nickel-nitrilotriacetic acid (Ni-NTA) agarose resin (TaKaRa, Beijing, China). SDS-PAGE and Western blot analysis were performed based on the methods of our lab (99, 101).

bioRxiv preprint doi: https://doi.org/10.1101/499871; this version posted December 19, 2018. The copyright holder for this preprint (which was not certified by peer review) is the author/funder, who has granted bioRxiv a license to display the preprint in perpetuity. It is made available under aCC-BY 4.0 International license.

Cell culture. Macrophage RAW264.7 cells were purchased from the Cell Bank of the Chinese Academy of Sciences (Shanghai, China), cultivated in DMEM medium supplemented with antibiotics (100 U/mL penicillin and 100 mg/mL streptomycin) and 10% FBS and incubated at 37 °C in a 5% CO_2 incubator. Cells were seeded at 2 × 10^5 cells per well in 24- or 96-well microplates and were incubated in 5% CO_2 at 37 °C.

Cell viability. Methylene blue uptake assay was performed to assess the effect of rFIP-glu on the viability of macrophage RAW264.7 cells (102). Briefly, Raw264.7 cells were incubated for 24 h, and then were incubated with rFIP-glu at different concentration (1, 2, 4 and 8 μg/mL), LPS (1 μg/mL) and Concanavalin A (ConA) (5 μg/mL) for 24 h. LPS and ConA were used as positive controls. The culture supernatant was discarded and cells were stained by adding 50 μL of 0.6% methylene blue to each well. Plates were incubated at 37 °C for 60 min, and then inverted to drain the stain solution away. Wells were washed with phosphate buffered saline (PBS) to remove unbound stain. Plates were air-dried for several minutes. Stained cells were solubilized by adding 50 μL of Elution Buffer (Ethanol : PBS : Acetic acid = 50 : 49 : 1 (Volume)) for 20 min with a gentle shake. The absorbance value was measured at 570 nm using a microplate reader (BIO-TEK®, USA) and the viability was expressed as percentage versus control group.

bioRxiv preprint doi: https://doi.org/10.1101/499871; this version posted December 19, 2018. The copyright holder for this preprint (which was not certified by peer review) is the author/funder, who has granted bioRxiv a license to display the preprint in perpetuity. It is made available under aCC-BY 4.0 International license.

422 **Phagocytosis assay.** Phagocytosis assay was measured by Neutral red uptake
423 assay (42). Briefly, Raw264.7 cells were incubated for 24 h, and then incubated with
424 rFIP-glu at different concentration (1, 2, 4 and 8 μg/mL) and ConA (5 μg/mL) for 24 h.
425 After the supernatant was discarded, 100 μL neutral red staining solution was added
426 into each well and the plates were continued to incubate for 30 min. The supernatant
427 was discarded and the cells were washed with PBS thrice to move free neutral red.
428 200 μL of cell lysis buffer (Ethanol : Acetic acid = 1 : 1 (Volume)) was added into
429 each well and the plates were shaken for 2 h at room temperature. The absorbance
430 value was measured at 540 nm using a microplate reader (BIO-TEK®, USA) and the
431 phagocytosis was expressed as OD values.
432
433 **Measurement of NO.** Raw264.7 cells were incubated for 24 h, and then were
434 incubated with rFIP-glu at different concentration (1, 2, 4 and 8 μg/mL) and LPS (1
435 μg/mL) for 24 h. The supernatants were used to evaluate NO production using Griess
436 assay by a NO Assay kit (Beyotime, Shanghai, China). According to the
437 manufacturer's protocol, sodium nitrite ($NaNO_2$) was used to generate a standard
438 curve to calculate the NO concentration.
439
440 **RNA extraction, sequencing and bioinformatics analysis.** Macrophage
441 RAW264.7 cells were cultured with rFIP-glu (4 μg/mL) for 6 h. Cells were harvested
442 and total RNA was extracted using TaKaRa MiniBEST Universal RNA Extraction Kit
443 (Beijing, China). Sequencing library was generated using Illumina Truseq stranded

bioRxiv preprint doi: https://doi.org/10.1101/499871; this version posted December 19, 2018. The copyright holder for this preprint (which was not certified by peer review) is the author/funder, who has granted bioRxiv a license to display the preprint in perpetuity. It is made available under aCC-BY 4.0 International license.

444 total RNA LT kit. On average 20 million Illumina paired-end reads (150 bp) were
445 generated for each sample. The reads were mapped to reference using Hisat and
446 differential expression analysis was performed using the R package DESeq2. In
447 addition, principle component analysis (PCA) was carried out on the genes
448 significantly expressed between all different groups. We combined results of two
449 Enrichment analysis tools. One was derived from GSEA 3.0 desktop by mapping all
450 genes to biological process of GO knowledge base and KEGG knowledge base. The
451 other was calculated by IPA (version 01-13) of which cutoff was FDR $\leq$ 0.001 and
452 Log2FoldChange > 1. The data were also analyzed on the free online platform of
453 Majorbio I-Sanger Cloud Platform (www.i-sanger.com).
454
455 **cDNA synthesis and Real-time quantitative PCR (RT-qPCR).** cDNA
456 was synthesized from 1 μg RNA using PrimeScript™ RT Master Mix (Perfect Real
457 Time) (TaKaRa, Beijing, China) according to the manufacturer's protocol. RT-qPCR
458 was performed using SYBR qPCR Master Mix (Vazyme, Nanjing, China) and Roche
459 LightCycler® 96 Application. For PCR, samples were heated to 95 °C for 1 min,
460 denatured at 95 °C for 20 s, annealed at 55 °C for 20 s, extended at 72 °C for 20 s, and
461 cycled 45 times. The primers in this study were listed in Table S1. All reactions were
462 performed in triplicate, and Ct values were normalized to β-actin. Relative expression
463 was calculated using the $2^{-\Delta\Delta Ct}$ method.
464
465 **Statistical analysis.** Graph Pad Prism 7 software was used to prepare graphs

bioRxiv preprint doi: https://doi.org/10.1101/499871; this version posted December 19, 2018. The copyright holder for this preprint (which was not certified by peer review) is the author/funder, who has granted bioRxiv a license to display the preprint in perpetuity. It is made available under aCC-BY 4.0 International license.

and statistical analysis. Data are expressed as means ± SD. The statistical analysis used One-way ANOVA analysis. Significance was indicated as ns, $p > 0.05$; ∗, $p \leq 0.05$; ∗∗, $p \leq 0.01$; ∗∗∗, $p \leq 0.001$; and ∗∗∗∗, $p \leq 0.0001$.

ACKNOWLEDGMENTS

This study was funded by the Tibet Shenglong Industry Co., Ltd. (No. 2013310031001210).

REFERENCE

1. Zhou XW, Su KQ, Zhang YM. 2012. Applied modern biotechnology for cultivation of *Ganoderma* and development of their products. Appl Microbiol Biotechnol 93:941-963.

2. El Enshasy HA, Hatti-Kaul R. 2013. Mushroom immunomodulators: unique molecules with unlimited applications. Trends Biotechnol 31:668-677.

3. Bastiaan-Net S, Chanput W, Hertz A, Zwittink RD, Mes JJ, Wichers HJ. 2013. Biochemical and functional characterization of recombinant fungal immunomodulatory proteins (rFIPs). Int Immunopharmacol 15:167-175.

4. Lin JW, Guan SY, Duan ZW, Shen YH, Fan WL, Chen LJ, Zhang L, Zhang L, Li TL. 2016. Gene cloning of a novel fungal immunomodulatory protein from *Chroogomphis rutilus* and its expression in *Pichia pastoris*. J Chem Technol Biotechnol 91:2761-2768.

5. Li S, Jiang Z, Sun L, Liu X, Huang Y, Wang F, Xin F. 2017. Characterization of a new fungal immunomodulatory protein, FIP-dsq2 from *Dichomitus*

bioRxiv preprint doi: https://doi.org/10.1101/499871; this version posted December 19, 2018. The copyright holder for this preprint (which was not certified by peer review) is the author/funder, who has granted bioRxiv a license to display the preprint in perpetuity. It is made available under aCC-BY 4.0 International license.

squalens. J Biotechnol 246:45-51.

6. Li S, Jiang Z, Xu W, Xie Y, Zhao L, Tang X, Wang F, Xin F. 2017. FIP-sch2, a new fungal immunomodulatory protein from *Stachybotrys chlorohalonata*, suppresses proliferation and migration in lung cancer cells. Appl Microbiol Biotechnol 101:3227-3235.

7. Li QZ, Wang XF, Zhou XW. 2011. Recent status and prospects of the fungal immunomodulatory protein family. Crit Rev Biotechnol 31:365-375.

8. Liao CH, Hsiao YM, Sheu GT, Chang JT, Wang PH, Wu MF, Shieh GJ, Hsu CP, Ko JL. 2007. Nuclear translocation of telomerase reverse transcriptase and calcium signaling in repression of telomerase activity in human lung cancer cells by fungal immunomodulatory protein from *Ganoderma tsugae*. Biochem Pharmacol 74:1541-1554.

9. Haendeler J, Hoffmann J, Brandes RP, Zeiher AM, Dimmeler S. 2003. Hydrogen peroxide triggers nuclear export of telomerase reverse transcriptase *via* Src kinase family-dependent phosphorylation of tyrosine 707. Mol Cell Biol 23:4598-4610.

10. Chiu LY, Hu ME, Yang TY, Hsin IL, Ko JL, Tsai KJ, Sheu GT. 2015. Immunomodulatory protein from *Ganoderma microsporum* induces pro-death autophagy through Akt-mTOR-p70S6K pathway inhibition in multidrug resistant lung cancer cells. PLoS One 10:e0125774.

11. Hsin IL, Hsu JC, Wu WJ, Lu HJ, Wu MF, Ko JL. 2018. GMI, a fungal immunomodulatory protein from *Ganoderma microsporum*, induce apoptosis

bioRxiv preprint doi: https://doi.org/10.1101/499871; this version posted December 19, 2018. The copyright holder for this preprint (which was not certified by peer review) is the author/funder, who has granted bioRxiv a license to display the preprint in perpetuity. It is made available under aCC-BY 4.0 International license.

via beta-catenin suppression in lung cancer cells. Environ Toxicol 33:955-961.

12. Lee YT, Wu CT, Sun HL, Ko JL, Lue KH. 2017. Fungal immunomodulatory protein-fve could modulate airway remodel through by affect IL17 cytokine. J Microbiol Immunol Infect 51:598-607.

13. Li SY, Shi LJ, Ding Y, Nie Y, Tang XM. 2015. Identification and functional characterization of a novel fungal immunomodulatory protein from *Postia placenta*. Food Chem Toxicol 78:64-70.

14. Xu H, Kong YY, Chen X, Guo MY, Bai XH, Lu YJ, Li W, Zhou XW. 2016. Recombinant FIP-gat, a fungal immunomodulatory protein from *Ganoderma atrum*, induces growth inhibition and cell death in breast cancer cells. J Agric Food Chem 64:2690-2698.

15. Chu PY, Sun HL, Ko JL, Ku MS, Lin LJ, Lee YT, Liao PF, Pan HH, Lu HL, Lue KH. 2017. Oral fungal immunomodulatory protein-*Flammulina velutipes* has influence on pulmonary inflammatory process and potential treatment for allergic airway disease: a mouse model. J Microbiol Immunol Infect 50:297-306.

16. Lee YT, Lee SS, Sun HL, Lu KH, Ku MS, Sheu JN, Ko JL, Lue KH. 2013. Effect of the fungal immunomodulatory protein FIP-fve on airway inflammation and cytokine production in mouse asthma model. Cytokine 61:237-244.

17. Liang C, Li H, Zhou H, Zhang S, Liu Z, Zhou Q, Sun F. 2012. Recombinant Lz-8 from *Ganoderma lucidum* induces endoplasmic reticulum

bioRxiv preprint doi: https://doi.org/10.1101/499871; this version posted December 19, 2018. The copyright holder for this preprint (which was not certified by peer review) is the author/funder, who has granted bioRxiv a license to display the preprint in perpetuity. It is made available under aCC-BY 4.0 International license.

533 stress-mediated autophagic cell death in SGC-7901 human gastric cancer cells.
534 Oncol Rep 27:1079-1089.
535 18. Davies LC, Jenkins SJ, Allen JE, Taylor PR. 2013. Tissue-resident
536 macrophages. Nat Immunol 14:986-995.
537 19. Sica A, Erreni M, Allavena P, Porta C. 2015. Macrophage polarization in
538 pathology. Cell Mol Life Sci 72:4111-4126.
539 20. Nonnenmacher Y, Hiller K. 2018. Biochemistry of proinflammatory
540 macrophage activation. Cell Mol Life Sci 75:2093-2109.
541 21. Vergadi E, Ieronymaki E, Lyroni K, Vaporidi K, Tsatsanis C. 2017. Akt
542 signaling pathway in macrophage activation and M1/M2 polarization. J
543 Immunol 198:1006-1014.
544 22. Galvan-Pena S, O'Neill LA. 2014. Metabolic reprograming in macrophage
545 polarization. Front Immunol 5:420.
546 23. Bashir S, Sharma Y, Elahi A, Khan F. 2016. Macrophage polarization: the link
547 between inflammation and related diseases. Inflamm Res 65:1-11.
548 24. Zhang Y, Liu D, Fang L, Zhao X, Zhou A, Xie J. 2018. A galactomannoglucan
549 derived from Agaricus brasiliensis: purification, characterization and
550 macrophage activation *via* MAPK and IkappaB/NFkappaB pathways. Food
551 Chem 239:603-611.
552 25. Schett G, Neurath MF. 2018. Resolution of chronic inflammatory disease:
553 universal and tissue-specific concepts. Nat Commun 9:3261.
554 26. Shapouri-Moghaddam A, Mohammadian S, Vazini H, Taghadosi M, Esmaeili

bioRxiv preprint doi: https://doi.org/10.1101/499871; this version posted December 19, 2018. The copyright holder for this preprint (which was not certified by peer review) is the author/funder, who has granted bioRxiv a license to display the preprint in perpetuity. It is made available under aCC-BY 4.0 International license.

SA, Mardani F, Seifi B, Mohammadi A, Afshari JT, Sahebkar A. 2018. Macrophage plasticity, polarization, and function in health and disease. J Cell Physiol 233:6425-6440.

27. Kollmann TR, Levy O, Montgomery RR, Goriely S. 2012. Innate immune function by Toll-like receptors: distinct responses in newborns and the elderly. Immunity 37:771-783.

28. Hug H, Mohajeri MH, La Fata G. 2018. Toll-like receptors: regulators of the immune response in the human gut. Nutrients 10:203.

29. Zhu L, Jones C, Zhang G. 2018. The role of phospholipase C signaling in macrophage-mediated inflammatory response. J Immunol Res 2018:5201759.

30. Wang DD, Pan WJ, Mehmood S, Chen XD, Chen Y. 2018. Polysaccharide isolated from *Sarcodon aspratus* induces RAW264.7 activity *via* TLR4-mediated NF-kappaB and MAPK signaling pathways. Int J Biol Macromol 120:1039-1047.

31. Yu T, Gao M, Yang P, Liu D, Wang D, Song F, Zhang X, Liu Y. 2018. Insulin promotes macrophage phenotype transition through PI3K/Akt and PPAR-gamma signaling during diabetic wound healing. J Cell Physiol doi:10.1002/jcp.27185.

32. Lim JE, Chung E, Son Y. 2017. A neuropeptide, Substance-P, directly induces tissue-repairing M2 like macrophages by activating the PI3K/Akt/mTOR pathway even in the presence of IFNγ. Sci Rep 7:9417.

33. Song M, Han L, Chen FF, Wang D, Wang F, Zhang L, Wang ZH, Zhong M,

bioRxiv preprint doi: https://doi.org/10.1101/499871; this version posted December 19, 2018. The copyright holder for this preprint (which was not certified by peer review) is the author/funder, who has granted bioRxiv a license to display the preprint in perpetuity. It is made available under aCC-BY 4.0 International license.

577 Tang MX, Zhang W. 2018. Adipocyte-derived exosomes carrying sonic
578 hedgehog mediate M1 macrophage polarization-induced insulin resistance *via*
579 Ptch and PI3K pathways. Cell Physiol Biochem 48:1416-1432.
580 34. Ren D, Lin D, Alim A, Zheng Q, Yang X. 2017. Chemical characterization of
581 a novel polysaccharide ASKP-1 from *Artemisia sphaerocephala* Krasch seed
582 and its macrophage activation *via* MAPK, PI3k/Akt and NF-kappaB signaling
583 pathways in RAW264.7 cells. Food Funct 8:1299-1312.
584 35. Zhao Y, Wang CL, Li RM, Hui TQ, Su YY, Yuan Q, Zhou XD, Ye L. 2014.
585 Wnt5a promotes inflammatory responses *via* nuclear factor kappaB
586 (NF-kappaB) and mitogen-activated protein kinase (MAPK) pathways in
587 human dental pulp cells. J Biol Chem 289:21028-21039.
588 36. Wang W, Liu P, Hao C, Wu L, Wan W, Mao X. 2017.
589 Neoagaro-oligosaccharide monomers inhibit inflammation in LPS-stimulated
590 macrophages through suppression of MAPK and NF-kappaB pathways. Sci
591 Rep 7:44252.
592 37. Liu Q, Xiao XH, Hu LB, Jie HY, Wang Y, Ye WC, Li MM, Liu Z. 2017.
593 Anhuienoside C ameliorates collagen-induced arthritis through inhibition of
594 MAPK and NF-kappaB signaling pathways. Front Pharmacol 8:299.
595 38. Sica A, Mantovani A. 2012. Macrophage plasticity and polarization: *in vivo*
596 veritas. J Clin Invest 122:787-795.
597 39. Tanaka S, Ko K, Kino K, Tsuchiya K, Yamashita A, Murasugi A, Sakuma S,
598 Tsunoo H. 1989. Complete amino acid sequence of an immunomodulatory

bioRxiv preprint doi: https://doi.org/10.1101/499871; this version posted December 19, 2018. The copyright holder for this preprint (which was not certified by peer review) is the author/funder, who has granted bioRxiv a license to display the preprint in perpetuity. It is made available under aCC-BY 4.0 International license.

protein, ling zhi-8 (LZ-8). An immunomodulator from a fungus, *Ganoderma lucidium*, having similarity to immunoglobulin variable regions. J Biol Chem 264:16372-16377.

40. Kino K, Yamashita A, Yamaoka K, Watanabe J, Tanaka S, Ko K, Shimizu K, Tsunoo H. 1989. Isolation and characterization of a new immunomodulatory protein, ling zhi-8 (LZ-8), from *Ganoderma lucidium*. J Biol Chem 264:472-478.

41. Aderem A, Underhill DM. 1999. Mechanisms of phagocytosis in macrophages. Annu Rev Immunol 17:593-623.

42. Xiong L, Ouyang KH, Jiang Y, Yang ZW, Hu WB, Chen H, Wang N, Liu X, Wang WJ. 2018. Chemical composition of *Cyclocarya paliurus* polysaccharide and inflammatory effects in lipopolysaccharide-stimulated RAW264.7 macrophage. Int J Biol Macromol 107:1898-1907.

43. Zhang M, Tian X, Wang Y, Wang D, Li W, Chen L, Pan W, Mehmood S, Chen Y. 2018. Immunomodulating activity of the polysaccharide TLH-3 from Tricholomalobayense in RAW264.7 macrophages. Int J Biol Macromol 107:2679-2685.

44. Wu W, Zhang M, Ren Y, Cai X, Yin Z, Zhang X, Min T, Wu H. 2017. Characterization and immunomodulatory activity of a novel peptide, ECFSTA, from wheat germ globulin. J Agric Food Chem 65:5561-5569.

45. Sheu F, Chien PJ, Hsieh KY, Chin KL, Huang WT, Tsao CY, Chen YF, Cheng HC, Chang HH. 2009. Purification, cloning, and functional characterization of

bioRxiv preprint doi: https://doi.org/10.1101/499871; this version posted December 19, 2018. The copyright holder for this preprint (which was not certified by peer review) is the author/funder, who has granted bioRxiv a license to display the preprint in perpetuity. It is made available under aCC-BY 4.0 International license.

a novel immunomodulatory protein from *Antrodia camphorata* (bitter mushroom) that exhibits TLR2-dependent NF-kappaB activation and M1 polarization within murine macrophages. J Agric Food Chem 57:4130-4141.

46. Shruthi RR, Venkatesh YP, Muralikrishna G. 2017. Structural and functional characterization of a novel immunomodulatory glycoprotein isolated from ajowan (*Trachyspermum ammi* L.). Glycoconj J 34:499-514.

47. Ahmad W, Jantan I, Kumolosasi E, Haque MA, Bukhari SNA. 2018. Immunomodulatory effects of *Tinospora crispa* extract and its major compounds on the immune functions of RAW 264.7 macrophages. Int Immunopharmacol 60:141-151.

48. Lu H, Zhang L, Zhao H, Li JJ, You HL, Jiang L, Hu JE. 2018. Activation of macrophages *in vitro* by phospholipids from brain of *Katsuwonus pelamis* (Skipjack Tuna). J Oleo Sci 67:327-333.

49. Ravetch JV, Bolland S. 2001. IgG Fc receptors. Annu Rev Immunol 19:275-290.

50. Joshi T, Butchar JP, Tridandapani S. 2006. Fcgamma receptor signaling in phagocytes. Int J Hematol 84:210-216.

51. Park JB. 2003. Phagocytosis induces superoxide formation and apoptosis in macrophages. Exp Mol Med 35:325-335.

52. Victor JR, Muniz BP, Fusaro AE, de Brito CA, Taniguchi EF, Duarte AJ, Sato MN. 2010. Maternal immunization with ovalbumin prevents neonatal allergy development and up-regulates inhibitory receptor Fc gamma RIIB expression

bioRxiv preprint doi: https://doi.org/10.1101/499871; this version posted December 19, 2018. The copyright holder for this preprint (which was not certified by peer review) is the author/funder, who has granted bioRxiv a license to display the preprint in perpetuity. It is made available under aCC-BY 4.0 International license.

643 on B cells. BMC Immunol 11:11.

644 53. Wu J, Lin R, Huang J, Guan W, Oetting WS, Sriramarao P, Blumenthal MN.
645 2014. Functional Fcgamma receptor polymorphisms are associated with
646 human allergy. PLoS One 9:e89196.

647 54. Burton OT, Epp A, Fanny ME, Miller SJ, Stranks AJ, Teague JE, Clark RA,
648 van de Rijn M, Oettgen HC. 2018. Tissue-specific expression of the
649 low-affinity IgG receptor, FcgammaRIIb, on human mast cells. Front Immunol
650 9:1244.

651 55. Burton OT, Tamayo JM, Stranks AJ, Koleoglou KJ, Oettgen HC. 2018.
652 Allergen-specific IgG antibody signaling through FcgammaRIIb promotes
653 food tolerance. J Allergy Clin Immunol 141:189-201. e3.

654 56. Billack B. 2006. Macrophage activation: role of toll-like receptors, nitric oxide,
655 and nuclear factor kappa B. Am J Pharm Educ 70:102.

656 57. Meng Y, Yan J, Yang G, Han Z, Tai G, Cheng H, Zhou Y. 2018. Structural
657 characterization and macrophage activation of a hetero-galactan isolated from
658 *Flammulina velutipes*. Carbohydr Polym 183:207-218.

659 58. Moreno-Fierros L, Garcia-Hernandez AL, Ilhuicatzi-Alvarado D,
660 Rivera-Santiago L, Torres-Martinez M, Rubio-Infante N, Legorreta-Herrera M.
661 2013. Cry1Ac protoxin from *Bacillus thuringiensis* promotes macrophage
662 activation by upregulating CD80 and CD86 and by inducing IL-6, MCP-1 and
663 TNF-alpha cytokines. Int Immunopharmacol 17:1051-1066.

664 59. Lull C, Wichers HJ, Savelkoul HF. 2005. Antiinflammatory and

bioRxiv preprint doi: https://doi.org/10.1101/499871; this version posted December 19, 2018. The copyright holder for this preprint (which was not certified by peer review) is the author/funder, who has granted bioRxiv a license to display the preprint in perpetuity. It is made available under aCC-BY 4.0 International license.

immunomodulating properties of fungal metabolites. Mediators Inflamm 2005:63-80.

60. Chang HH, Yeh CH, Sheu F. 2009. A novel immunomodulatory protein from *Poria cocos* induces Toll-like receptor 4-dependent activation within mouse peritoneal macrophages. J Agric Food Chem 57:6129-6139.

61. Ng A, Tam WW, Zhang MW, Ho CS, Husain SF, McIntyre RS, Ho RC. 2018. IL-1beta, IL-6, TNF-alpha and CRP in elderly patients with depression or Alzheimer's disease: systematic review and meta-analysis. Sci Rep 8:12050.

62. Deshmane SL, Kremlev S, Amini S, Sawaya BE. 2009. Monocyte chemoattractant protein-1 (MCP-1): an overview. J Interferon Cytokine Res 29:313-326.

63. Daly C, Rollins BJ. 2003. Monocyte chemoattractant protein-1 (CCL2) in inflammatory disease and adaptive immunity: therapeutic opportunities and controversies. Microcirculation 10:247-257.

64. Khallou-Laschet J, Varthaman A, Fornasa G, Compain C, Gaston AT, Clement M, Dussiot M, Levillain O, Graff-Dubois S, Nicoletti A, Caligiuri G. 2010. Macrophage plasticity in experimental atherosclerosis. PLoS One 5:e8852.

65. Ming XF, Rajapakse AG, Yepuri G, Xiong Y, Carvas JM, Ruffieux J, Scerri I, Wu Z, Popp K, Li J, Sartori C, Scherrer U, Kwak BR, Montani JP, Yang Z. 2012. Arginase II promotes macrophage inflammatory responses through mitochondrial reactive oxygen species, contributing to insulin resistance and atherogenesis. J Am Heart Assoc 1:e000992.

bioRxiv preprint doi: https://doi.org/10.1101/499871; this version posted December 19, 2018. The copyright holder for this preprint (which was not certified by peer review) is the author/funder, who has granted bioRxiv a license to display the preprint in perpetuity. It is made available under aCC-BY 4.0 International license.

687 66. Fauskanger M, Haabeth OAW, Skjeldal FM, Bogen B, Tveita AA. 2018.
688 Tumor killing by CD4(+) T cells is mediated *via* induction of inducible nitric
689 oxide synthase-dependent macrophage cytotoxicity. Front Immunol 9:1684.
690 67. Villalta SA, Rinaldi C, Deng B, Liu G, Fedor B, Tidball JG. 2011.
691 Interleukin-10 reduces the pathology of mdx muscular dystrophy by
692 deactivating M1 macrophages and modulating macrophage phenotype. Hum
693 Mol Genet 20:790-805.
694 68. Mahon OR, O'Hanlon S, Cunningham CC, McCarthy GM, Hobbs C, Nicolosi
695 V, Kelly DJ, Dunne A. 2018. Orthopaedic implant materials drive M1
696 macrophage polarization in a spleen tyrosine kinase- and mitogen-activated
697 protein kinase-dependent manner. Acta Biomater 65:426-435.
698 69. Kim B, Kim EY, Lee EJ, Han JH, Kwak CH, Jung YS, Lee SO, Chung TW,
699 Ha KT. 2018. Panax notoginseng inhibits tumor growth through activating
700 macrophage to M1 polarization. Am J Chin Med 46:1369-1385.
701 70. Tian L, Li W, Yang L, Chang N, Fan X, Ji X, Xie J, Yang L, Li L. 2017.
702 Cannabinoid receptor 1 participates in liver inflammation by promoting M1
703 macrophage polarization *via* RhoA/NF-kappaB p65 and ERK1/2 pathways,
704 respectively, in mouse liver fibrogenesis. Front Immunol 8:1214.
705 71. Pachulec E, Abdelwahed Bagga RB, Chevallier L, O'Donnell H, Guillas C,
706 Jaubert J, Montagutelli X, Carniel E, Demeure CE. 2017. Enhanced
707 macrophage M1 polarization and resistance to apoptosis enable resistance to
708 plague. J Infect Dis 216:761-770.

bioRxiv preprint doi: https://doi.org/10.1101/499871; this version posted December 19, 2018. The copyright holder for this preprint (which was not certified by peer review) is the author/funder, who has granted bioRxiv a license to display the preprint in perpetuity. It is made available under aCC-BY 4.0 International license.

709 72. Lehmann JM, Claus K, Jansen C, Pohlmann A, Schierwagen R, Meyer C,
710 Thomas D, Manekeller S, Claria J, Strassburg CP, Trautwein C, Wasmuth HE,
711 Berres ML, Trebicka J. 2018. Circulating CXCL10 in cirrhotic portal
712 hypertension might reflect systemic inflammation and predict ACLF and
713 mortality. Liver Int 38:875-884.
714 73. Wasmuth HE, Tacke F, Trautwein C. 2010. Chemokines in liver inflammation
715 and fibrosis. Semin Liver Dis 30:215-225.
716 74. Qin Y, Sun X, Shao X, Cheng C, Feng J, Sun W, Gu D, Liu W, Xu F, Duan Y.
717 2015. Macrophage-microglia networks drive M1 microglia polarization after
718 mycobacterium infection. Inflammation 38:1609-1616.
719 75. Matsui M, Adib-Conquy M, Coste A, Kumar-Roine S, Pipy B, Laurent D,
720 Pauillac S. 2012. Aqueous extract of *Vitex trifolia* L. (Labiatae) inhibits
721 LPS-dependent regulation of inflammatory mediators in RAW 264.7
722 macrophages through inhibition of Nuclear Factor kappa B translocation and
723 expression. J Ethnopharmacol 143:24-32.
724 76. Ashley JW, Hancock WD, Nelson AJ, Bone RN, Tse HM, Wohltmann M, Turk
725 J, Ramanadham S. 2016. Polarization of macrophages toward M2 phenotype
726 is favored by reduction in iPLA2beta (Group VIA phospholipase A2). J Biol
727 Chem 291:23268-23281.
728 77. Cheng Y, Yang C, Luo D, Li X, Le XC, Rong J. 2018. N-propargyl caffeamide
729 skews macrophages towards a resolving M2-like phenotype against
730 myocardial ischemic injury *via* activating Nrf2/HO-1 pathway and inhibiting

bioRxiv preprint doi: https://doi.org/10.1101/499871; this version posted December 19, 2018. The copyright holder for this preprint (which was not certified by peer review) is the author/funder, who has granted bioRxiv a license to display the preprint in perpetuity. It is made available under aCC-BY 4.0 International license.

731 NF-kB pathway. Cell Physiol Biochem 47:2544-2557.

732 78. Lu CL, Wei Z, Min W, Hu MM, Chen WL, Xu XJ, Lu CJ. 2015.
733 Polysaccharides from *Smilax glabra* inhibit the pro-inflammatory mediators
734 *via* ERK1/2 and JNK pathways in LPS-induced RAW264.7 cells. Carbohydr
735 Polym 122:428-436.

736 79. Tran PL, Tran PT, Tran HNK, Lee S, Kim O, Min BS, Lee JH. 2018. A
737 prenylated flavonoid, 10-oxomornigrol F, exhibits anti-inflammatory effects
738 by activating the Nrf2/heme oxygenase-1 pathway in macrophage cells. Int
739 Immunopharmacol 55:165-173.

740 80. Sheu F, Chien PJ, Chien AL, Chen YF, Chin KL. 2004. Isolation and
741 characterization of an immunomodulatory protein (APP) from the Jew's Ear
742 mushroom *Auricularia polytricha*. Food Chemistry 87:593-600.

743 81. Mitsi E, Kamng'ona R, Rylance J, Solorzano C, Jesus Reine J, Mwandumba
744 HC, Ferreira DM, Jambo KC. 2018. Human alveolar macrophages
745 predominately express combined classical M1 and M2 surface markers in
746 steady state. Respir Res 19:66.

747 82. Na YR, Je S, Seok SH. 2018. Metabolic features of macrophages in
748 inflammatory diseases and cancer. Cancer Lett 413:46-58.

749 83. Zhu Y, Li X, Chen J, Chen T, Shi Z, Lei M, Zhang Y, Bai P, Li Y, Fei X. 2016.
750 The pentacyclic triterpene Lupeol switches M1 macrophages to M2 and
751 ameliorates experimental inflammatory bowel disease. Int Immunopharmacol
752 30:74-84.

bioRxiv preprint doi: https://doi.org/10.1101/499871; this version posted December 19, 2018. The copyright holder for this preprint (which was not certified by peer review) is the author/funder, who has granted bioRxiv a license to display the preprint in perpetuity. It is made available under aCC-BY 4.0 International license.

753 84. Jang SE, Han MJ, Kim SY, Kim DH. 2014. *Lactobacillus plantarum*
754 CLP-0611 ameliorates colitis in mice by polarizing M1 to M2-like
755 macrophages. Int Immunopharmacol 21:186-192.
756 85. Yao J, Du Z, Li Z, Zhang S, Lin Y, Li H, Zhou L, Wang Y, Yan G, Wu X, Duan
757 Y, Du G. 2018. 6-Gingerol as an arginase inhibitor prevents urethane-induced
758 lung carcinogenesis by reprogramming tumor supporting M2 macrophages to
759 M1 phenotype. Food Funct 9:4611-4620.
760 86. Zhu Z, Scalfi-Happ C, Ryabova A, Grafe S, Wiehe A, Peter RU, Loschenov V,
761 Steiner R, Wittig R. 2018. Photodynamic activity of Temoporfin nanoparticles
762 induces a shift to the M1-like phenotype in M2-polarized macrophages. J
763 Photochem Photobiol B 185:215-222.
764 87. Yang Y, Xing RG, Liu S, Qin YK, Li KC, Yu HH, Li PC. 2018.
765 Immunostimulatory effects of sulfated chitosans on RAW 264.7 mouse
766 macrophages *via* the activation of PI3K/Akt signaling pathway. Int J Bio
767 Macromol 108:1310-1321.
768 88. Torres-Martinez M, Rubio-Infante N, Garcia-Hernandez AL, Nava-Acosta R,
769 Ilhuicatzi-Alvarado D, Moreno-Fierros L. 2016. Cry1Ac toxin induces
770 macrophage activation *via* ERK1/2, JNK and p38 mitogen-activated protein
771 kinases. Int J Biochem Cell Biol 78:106-115.
772 89. Solinas G, Becattini B. 2017. The role of PI3Kgamma in metabolism and
773 macrophage activation. Oncotarget 8:106145-106146.
774 90. Vidya MK, Kumar VG, Sejian V, Bagath M, Krishnan G, Bhatta R. 2018.

bioRxiv preprint doi: https://doi.org/10.1101/499871; this version posted December 19, 2018. The copyright holder for this preprint (which was not certified by peer review) is the author/funder, who has granted bioRxiv a license to display the preprint in perpetuity. It is made available under aCC-BY 4.0 International license.

775 Toll-like receptors: significance, ligands, signaling pathways, and functions in
776 mammals. Int Rev Immunol 37:20-36.
777 91. Hsieh YH, Deng JS, Chang YS, Huang GJ. 2018. Ginsenoside Rh2
778 ameliorates lipopolysaccharide-induced acute lung injury by regulating the
779 TLR4/PI3K/Akt/mTOR, Raf-1/MEK/ERK, and Keap1/Nrf2/HO-1 signaling
780 pathways in mice. Nutrients 10:1208.
781 92. Liu HT, Li WM, Li XY, Xu QS, Liu QS, Bai XF, Yu C, Du YG. 2010.
782 Chitosan oligosaccharides inhibit the expression of interleukin-6 in
783 lipopolysaccharide-induced human umbilical vein endothelial cells through
784 p38 and ERK1/2 protein kinases. Basic Clin Pharmacol Toxicol 106:362-371.
785 93. Sulistyowati E, Lee MY, Wu LC, Hsu JH, Dai ZK, Wu BN, Lin MC, Yeh JL.
786 2018. Exogenous heat shock cognate protein 70 suppresses LPS-induced
787 inflammation by down-regulating NF-kappaB through MAPK and MMP-2/-9
788 pathways in macrophages. Molecules 23:2124.
789 94. Li ST, Dai Q, Zhang SX, Liu YJ, Yu QQ, Tan F, Lu SH, Wang Q, Chen JW,
790 Huang HQ, Liu PQ, Li M. 2018. Ulinastatin attenuates LPS-induced
791 inflammation in mouse macrophage RAW264.7 cells by inhibiting the
792 JNK/NF-kappaB signaling pathway and activating the PI3K/Akt/Nrf2 pathway.
793 Acta Pharmacol Sin 39:1294-1304.
794 95. Hwangbo C, Lee HS, Park J, Choe J, Lee JH. 2009. The anti-inflammatory
795 effect of tussilagone, from *Tussilago farfara*, is mediated by the induction of
796 heme oxygenase-1 in murine macrophages. Int Immunopharmacol

bioRxiv preprint doi: https://doi.org/10.1101/499871; this version posted December 19, 2018. The copyright holder for this preprint (which was not certified by peer review) is the author/funder, who has granted bioRxiv a license to display the preprint in perpetuity. It is made available under aCC-BY 4.0 International license.

9:1578-1584.

96. Jaramillo MC, Zhang DD. 2013. The emerging role of the Nrf2-Keap1 signaling pathway in cancer. Genes Dev 27:2179-2191.

97. Zhao M, Chen J, Zhu P, Fujino M, Takahara T, Toyama S, Tomita A, Zhao L, Yang Z, Hei M, Zhong L, Zhuang J, Kimura S, Li XK. 2015. Dihydroquercetin (DHQ) ameliorated concanavalin A-induced mouse experimental fulminant hepatitis and enhanced HO-1 expression through MAPK/Nrf2 antioxidant pathway in RAW cells. Int Immunopharmacol 28:938-944.

98. Park EJ, Kim YM, Park SW, Kim HJ, Lee JH, Lee DU, Chang KC. 2013. Induction of HO-1 through p38 MAPK/Nrf2 signaling pathway by ethanol extract of *Inula helenium* L. reduces inflammation in LPS-activated RAW 264.7 cells and CLP-induced septic mice. Food Chem Toxicol 55:386-395.

99. Wang XF, Li QZ, Bao TW, Cong WR, Song WX, Zhou XW. 2013. *In vitro* rapid evolution of fungal immunomodulatory proteins by DNA family shuffling. Appl Microbiol Biotechnol 97:2455-2465.

100. Zhou X, Li Q, Zhao J, Tang K, Lin J, Yin Y. 2007. Comparison of rapid DNA extraction methods applied to PCR identification of medicinal mushroom *Ganoderma* spp. Prep Biochem Biotechnol 37:369-380.

101. Li QZ, Wang XF, Bao TW, Ran L, Lin J, Zhou XW. 2010. *In vitro* synthesis of a recombinant fungal immunomodulatory protein from Lingzhi or Reishi medicinal mushroom, *Ganoderma lucidum*. Int J Med Mushrooms

bioRxiv preprint doi: https://doi.org/10.1101/499871; this version posted December 19, 2018. The copyright holder for this preprint (which was not certified by peer review) is the author/funder, who has granted bioRxiv a license to display the preprint in perpetuity. It is made available under aCC-BY 4.0 International license.

12:347-358.

102. Ma G, Chong L, Li Z, Cheung AH, Tattersall MH. 2009. Anticancer activities of sesquiterpene lactones from Cyathocline purpurea *in vitro*. Cancer Chemother Pharmacol 64:143-152.

Figure legends

FIG 1 Production of rFIP-glu in *P. pastoris* GS115 cells. A, schematic map of the recombinant expression vector pPIC9K-glu-His. B, rFIP-glu detected by SDS-PAGE. C, Western blot analysis of rFIP-glu using anti-6×His tag. D, Western blot analysis of rFIP-glu using anti-rFIP-glu. Lane M: protein molecular mass marker. Lane 1, *P. pastoris* GS115 cells without being induced by MeOH. Lane 2, *P. pastoris* GS115 cells induced by MeOH. Lane 3, *P. pastoris* GS115 cells containing expression vector pPIC9K without being induced by MeOH. Lane 4, *P. pastoris* GS115 cells containing expression vector pPIC9K induced by MeOH. Lane 5, *P. pastoris* GS115 cells containing expression vector pPIC9K-glu-His without being induced by MeOH. Lane 6, *P. pastoris* GS115 cells containing expression vector pPIC9K-glu-His induced by MeOH.

FIG 2 Effect of rFIP-glu on the viability of RAW264.7 cells. RAW264.7 cells were treated with different concentration of rFIP-glu (1, 2, 4, 8, 16 and 32 μg/mL) or PBS (as control), Concanavalin A (ConA) and lipopolysaccharide (LPS) for 24 h. The cells were measured by methylene blue uptake assay. Data were expressed as means ± SD (n = 5). ns, $p > 0.05$; **, $p \leq 0.01$; ****, $p \leq 0.0001$ versus

bioRxiv preprint doi: https://doi.org/10.1101/499871; this version posted December 19, 2018. The copyright holder for this preprint (which was not certified by peer review) is the author/funder, who has granted bioRxiv a license to display the preprint in perpetuity. It is made available under aCC-BY 4.0 International license.

841 control group.

842 FIG 3 Effects of rFIP-glu on RAW264.7 cells phagocytosis. RAW264.7 cells were
843 treated with different concentration of rFIP-glu (1, 2, 4 and 8 μg/mL). Control
844 cells were treated with PBS only and ConA cells as positive control were treated
845 with 5 μg/mL. The effects were assessed by neutral red uptake assay. Data were
846 expressed as means ± SD (n = 3). ∗, $p \leq 0.05$ versus control group.

847 FIG 4 Effects of rFIP-glu on RAW264.7 cells. The cells were treated with different
848 concentration of rFIP-glu (1, 2, 4 and 8 μg/mL) for 6 h. The mRNA expression
849 of TNF-α (A), Arginase II (B), iNOS (C), MCP-1 (CCL-2) (D), IL-10 (E),
850 CXCL-10 (F) and IL-6 (G) was measured by qRT-PCR. Data were expressed as
851 means ± SD (n = 3). ns, $p > 0.05$; ∗∗, $p \leq 0.01$; ∗∗∗, $p \leq 0.001$; ∗∗∗∗, $p \leq 0.0001$
852 versus control group.

853 FIG 5 Effects of rFIP-glu on LPS-induced RAW264.7 cells. Cells were treated with
854 different concentration of rFIP-glu (1, 2, 4 and 8 μg/mL) and LPS (1 μg/mL) and
855 incubated for 6 h. The mRNA expression of TNF-α (A), MCP-1 (CCL-2) (B),
856 Arginase II (C), IL-10 (D), IL-1β (E), IL-6 (F) and CXCL-10 (G) was measured
857 by qRT-PCR. Data were expressed as means ± SD (n = 3). ####, $p \leq 0.0001$
858 versus control group. ns, $p > 0.05$; ∗∗, $p \leq 0.01$; ∗∗∗, $p \leq 0.001$; ∗∗∗∗, $p \leq 0.0001$
859 versus LPS group. The content of NO (H) in cell supernatant was determined by
860 Griess assay. Values are means ± SD (n = 5). ####, $p \leq 0.0001$ versus control
861 group. ∗∗, $p \leq 0.01$; ∗∗∗∗, $p \leq 0.0001$ versus LPS group.

862 FIG 6 RNA-seq analysis of macrophage RAW264.7 cells. (A) Principle component

bioRxiv preprint doi: https://doi.org/10.1101/499871; this version posted December 19, 2018. The copyright holder for this preprint (which was not certified by peer review) is the author/funder, who has granted bioRxiv a license to display the preprint in perpetuity. It is made available under aCC-BY 4.0 International license.

863 analysis of RAW264.7 cells treated with and without rFIP-glu. (B) Heatmap of
864 RAW264.7 cells treated with and without rFIP-glu. (C) Scatter plots of
865 differentially expressed genes between PBS- and rFIP-glu-treated macrophages.
866 Up-regulated genes are depicted in red and down-regulated gene in green (FDR
867 ≤ 0.001, fold change > 1). (D) GO analysis of the differentially expressed genes.
868 (E) GO enrichment analysis of the differentially expressed genes. (F) KEGG
869 pathway enrichment analysis of the differentially expressed genes. (G)
870 Confirmation of RNA-seq results by qRT-PCR.

871 FIG 7 Effect of rFIP-glu on signaling pathways. RAW264.7 cells were pre-treated
872 with 50 μM of LY294002 for 30 min and then treated with 4 μg/ml of rFIP-glu
873 for 6 h. The mRNA expression of MCP-1 (CCL-2) (A) and TNF-α (B) was
874 measured by qRT-PCR. RAW264.7 cells were pre-treated with 20 μM of U0126,
875 30 μM of SP600125 or 10 μM of SB203580 for 30 min and then treated with 4
876 μg/ml of rFIP-glu for 6 h. The mRNA expression of TNF-α (D), MCP-1 (CCL-2)
877 (E) and iNOS (F) was measured by qRT-PCR. Data were expressed as means ±
878 SD (n = 3). ####, $p \leq 0.0001$ versus control group. ***, $p \leq 0.001$; ****, $p \leq$
879 0.0001 versus rFIP-glu group.

880 FIG 8 Possible immunomodulatory signaling mechanism of rFIP-glu in RAW264.7
881 macrophages.

882

883 ***Supplementary legends***

884 FIG S1 The effect of rFIP-glu on morphological changes of RAW264.7 cells.

bioRxiv preprint doi: https://doi.org/10.1101/499871; this version posted December 19, 2018. The copyright holder for this preprint (which was not certified by peer review) is the author/funder, who has granted bioRxiv a license to display the preprint in perpetuity. It is made available under aCC-BY 4.0 International license.

RAW264.6 cells were incubated with LPS, rFIP-glu or both for 6 h. Cells were subjected to microscopic analysis (200×). All experiments were performed in duplicates. The data from one representative experiment out of two independent experiments were shown. Bar is 50 μm. A, untreated cells. Untreated RAW 264.7 cells as control exhibited a round morphology. B, LPS-treated cells. LPS-treated RAW 264.7 cells exhibited changes of morphology including pseudopodia formation and cell spreading. C, rFIP-glu-treated cells. After stimulated by rFIP-glu, the volume of RAW 264.7 cells increased and agglutination happened. D, rFIP-glu and LPS-stimulated cells. rFIP-glu treatment reversed morphology change in LPS-stimulated RAW 264.7 cells, with increase in volume and agglutination.

FIG S2 Heatmap of Toll-like receptors pathway in RAW264.7 cells treated with and without rFIP-glu. RAW264.7 cells were treated with 4 μg/mL of rFIP-glu for 6 h.

FIG S3 Heatmap of MAPK receptors pathway in RAW264.7 cells treated with and without rFIP-glu. RAW264.7 cells were treated with 4 μg/mL of rFIP-glu for 6 h.

FIG S4 Heatmap of FcγR-mediated phagocytosis pathway in RAW264.7 cells treated with and without rFIP-glu. RAW264.7 cells were treated with 4 μg/mL of rFIP-glu for 6 h.

FIG S5 Effects of rFIP-glu on the mRNA level of TLR4 in RAW264.7 cells. The cells were treated with 4 μg/mL of rFIP-glu for 6 h. The mRNA expression of TLR4 was measured by qRT-PCR.

FIG S6 Effects of rFIP-glu on the mRNA level of HO-1 in RAW264.7 cells. The cells

bioRxiv preprint doi: https://doi.org/10.1101/499871; this version posted December 19, 2018. The copyright holder for this preprint (which was not certified by peer review) is the author/funder, who has granted bioRxiv a license to display the preprint in perpetuity. It is made available under aCC-BY 4.0 International license.

were treated with different concentrations of rFIP-glu (1, 2, 4 and 8 μg/mL) for 6 h. The mRNA expression of HO-1 was measured by qRT-PCR. Data were expressed as means ± SD (n = 3). ****, $p \leq 0.0001$ versus control group.

TABLE S1 Primers used in this study.

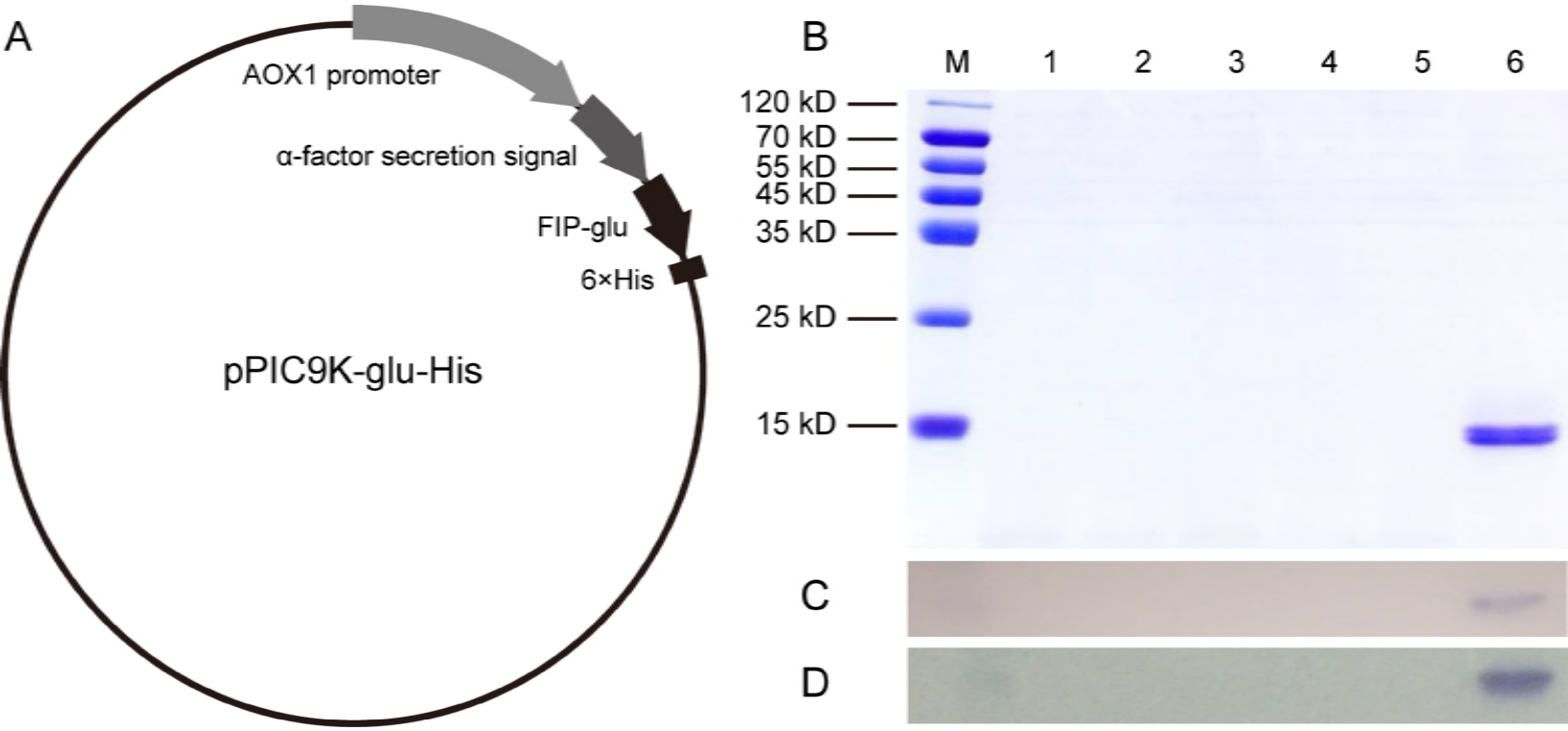
A
AOX1 promoter
α-factor secretion signal
FIP-glu
6×His
pPIC9K-glu-His
B
M
1
2
3
4
5
6
120 kD
70 kD
55 kD
45 kD
35 kD
25 kD
15 kD
C
D

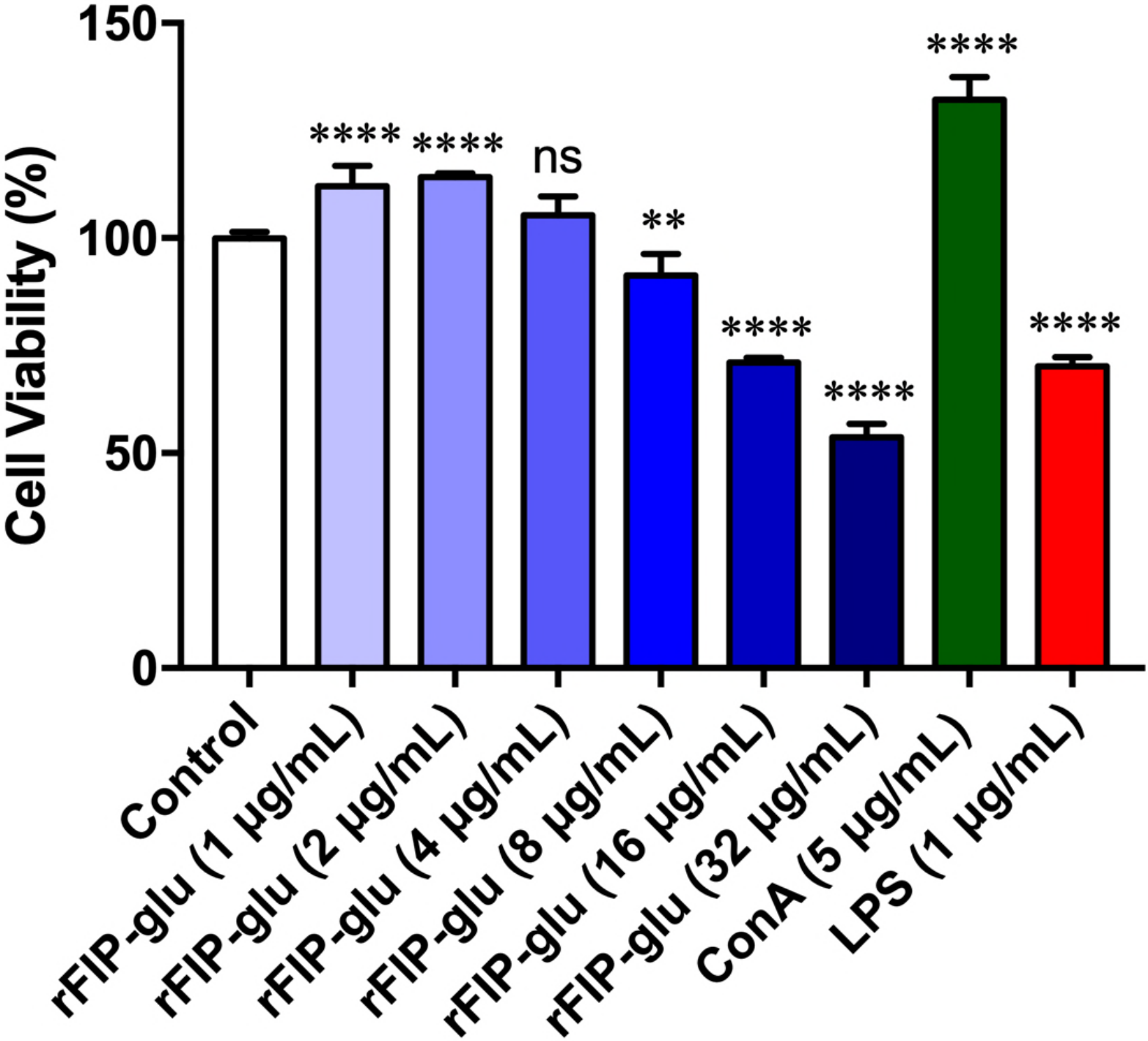
Cell Viability (%)
150
100
50
0
****
****
ns
**
****
****
****
****
Control
rFIP-glu (1 μg/mL)
rFIP-glu (2 μg/mL)
rFIP-glu (4 μg/mL)
rFIP-glu (8 μg/mL)
rFIP-glu (16 μg/mL)
rFIP-glu (32 μg/mL)
ConA (5 μg/mL)
LPS (1 μg/mL)

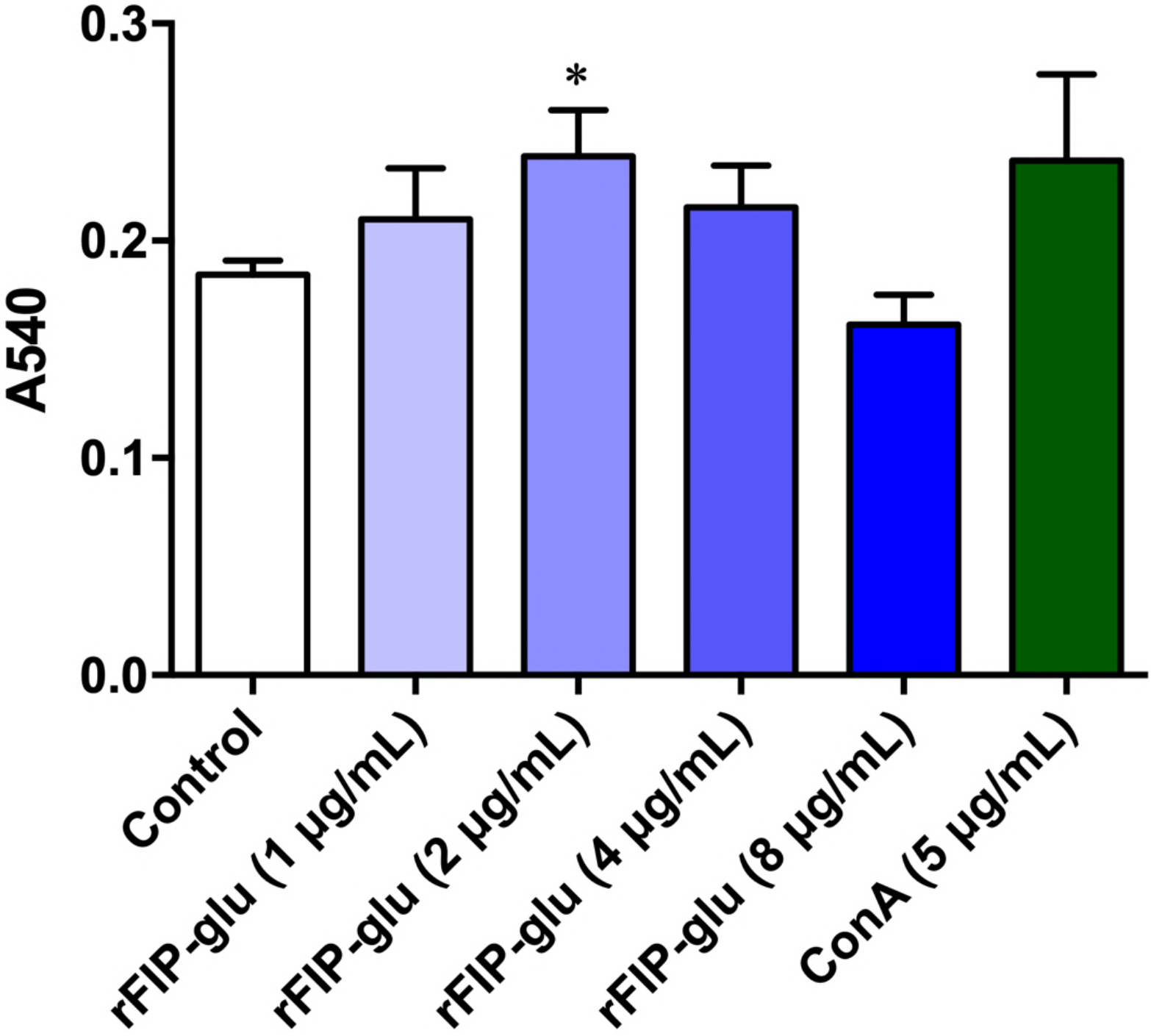
0.3
0.2
0.1
0.0
A540
*
Control
rFIP-glu (1 μg/mL)
rFIP-glu (2 μg/mL)
rFIP-glu (4 μg/mL)
rFIP-glu (8 μg/mL)
ConA (5 μg/mL)

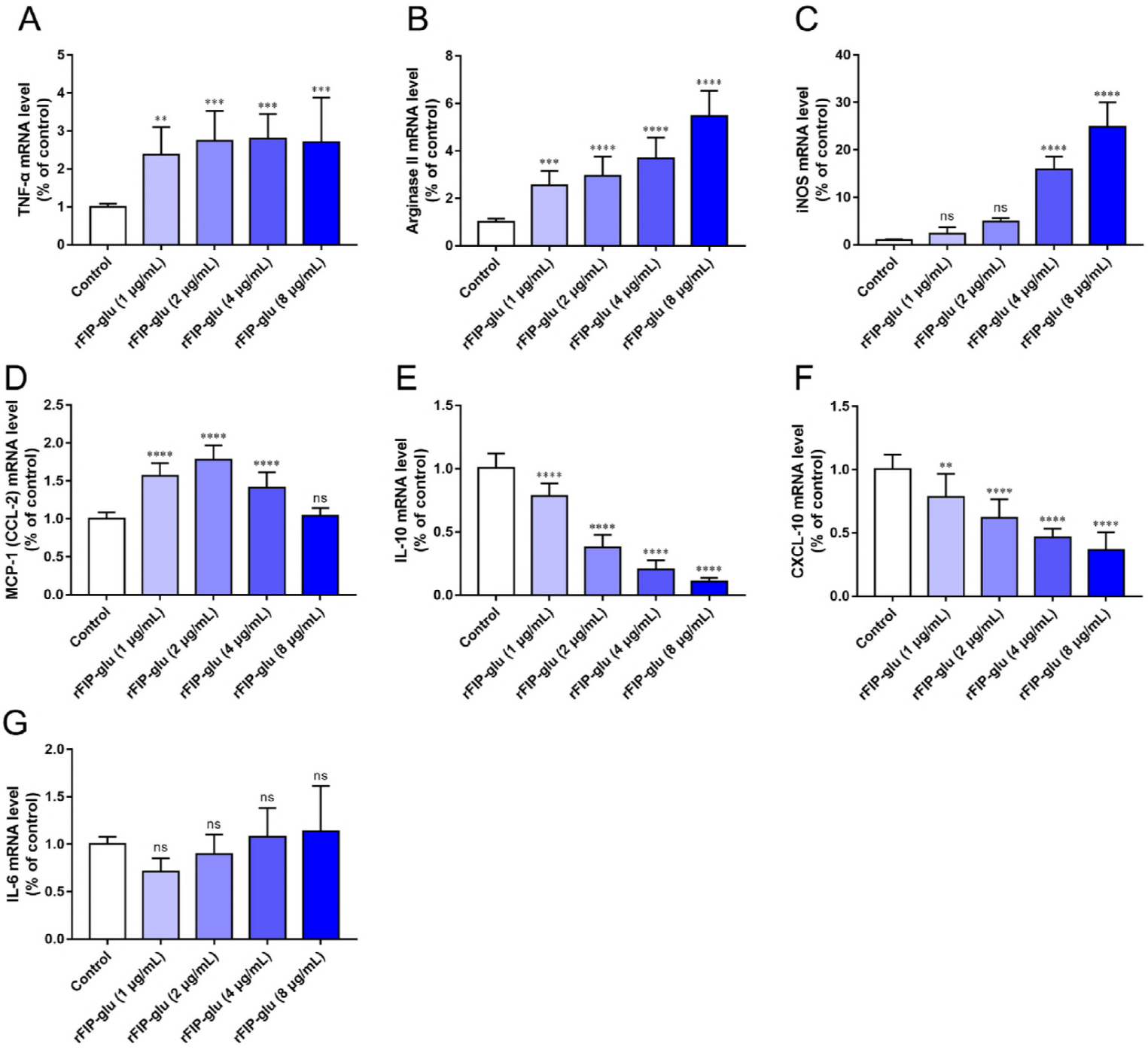
A
TNF-α mRNA level (% of control)
0
1
2
3
4
5
**
***
***
***
Control
rFIP-glu (1 μg/mL)
rFIP-glu (2 μg/mL)
rFIP-glu (4 μg/mL)
rFIP-glu (8 μg/mL)
B
Arginase II mRNA level (% of control)
0
2
4
6
8
***
****
****
****
Control
rFIP-glu (1 μg/mL)
rFIP-glu (2 μg/mL)
rFIP-glu (4 μg/mL)
rFIP-glu (8 μg/mL)
C
iNOS mRNA level (% of control)
0
10
20
30
40
ns
ns
****
****
Control
rFIP-glu (1 μg/mL)
rFIP-glu (2 μg/mL)
rFIP-glu (4 μg/mL)
rFIP-glu (8 μg/mL)
D
MCP-1 (CCL-2) mRNA level (% of control)
0.0
0.5
1.0
1.5
2.0
2.5
****
****
****
ns
Control
rFIP-glu (1 μg/mL)
rFIP-glu (2 μg/mL)
rFIP-glu (4 μg/mL)
rFIP-glu (8 μg/mL)
E
IL-10 mRNA level (% of control)
0.0
0.5
1.0
1.5
****
****
****
****
Control
rFIP-glu (1 μg/mL)
rFIP-glu (2 μg/mL)
rFIP-glu (4 μg/mL)
rFIP-glu (8 μg/mL)
F
CXCL-10 mRNA level (% of control)
0.0
0.5
1.0
1.5
**
****
****
****
Control
rFIP-glu (1 μg/mL)
rFIP-glu (2 μg/mL)
rFIP-glu (4 μg/mL)
rFIP-glu (8 μg/mL)
G
IL-6 mRNA level (% of control)
0.0
0.5
1.0
1.5
2.0
ns
ns
ns
ns
Control
rFIP-glu (1 μg/mL)
rFIP-glu (2 μg/mL)
rFIP-glu (4 μg/mL)
rFIP-glu (8 μg/mL)

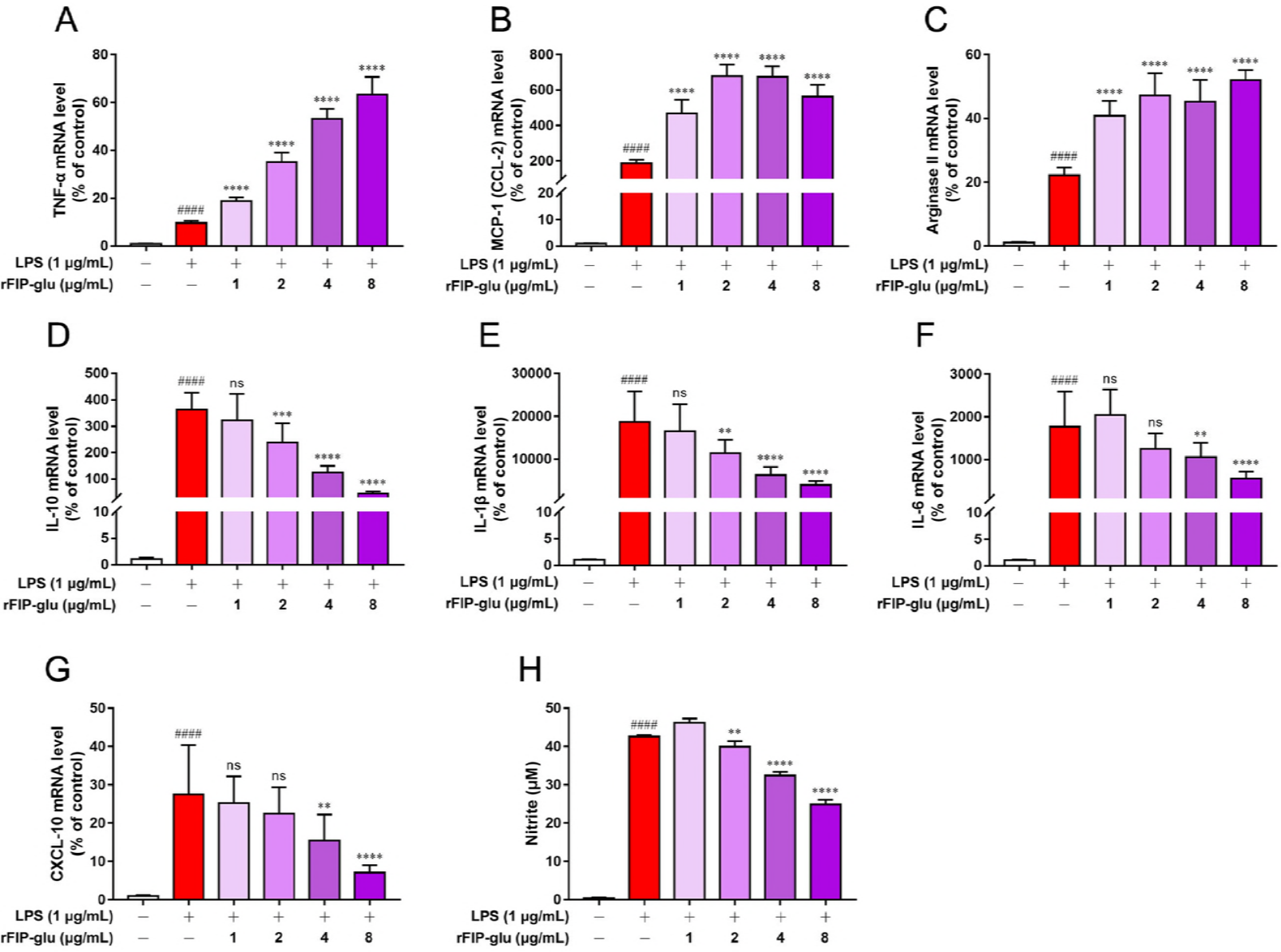
A
TNF-α mRNA level (% of control)
B
MCP-1 (CCL-2) mRNA level (% of control)
C
Arginase II mRNA level (% of control)
D
IL-10 mRNA level (% of control)
E
IL-1β mRNA level (% of control)
F
IL-6 mRNA level (% of control)
G
CXCL-10 mRNA level (% of control)
H
Nitrite (μM)
LPS (1 μg/mL) – + + + + +
rFIP-glu (μg/mL) – – 1 2 4 8
ns ** *** **** ****

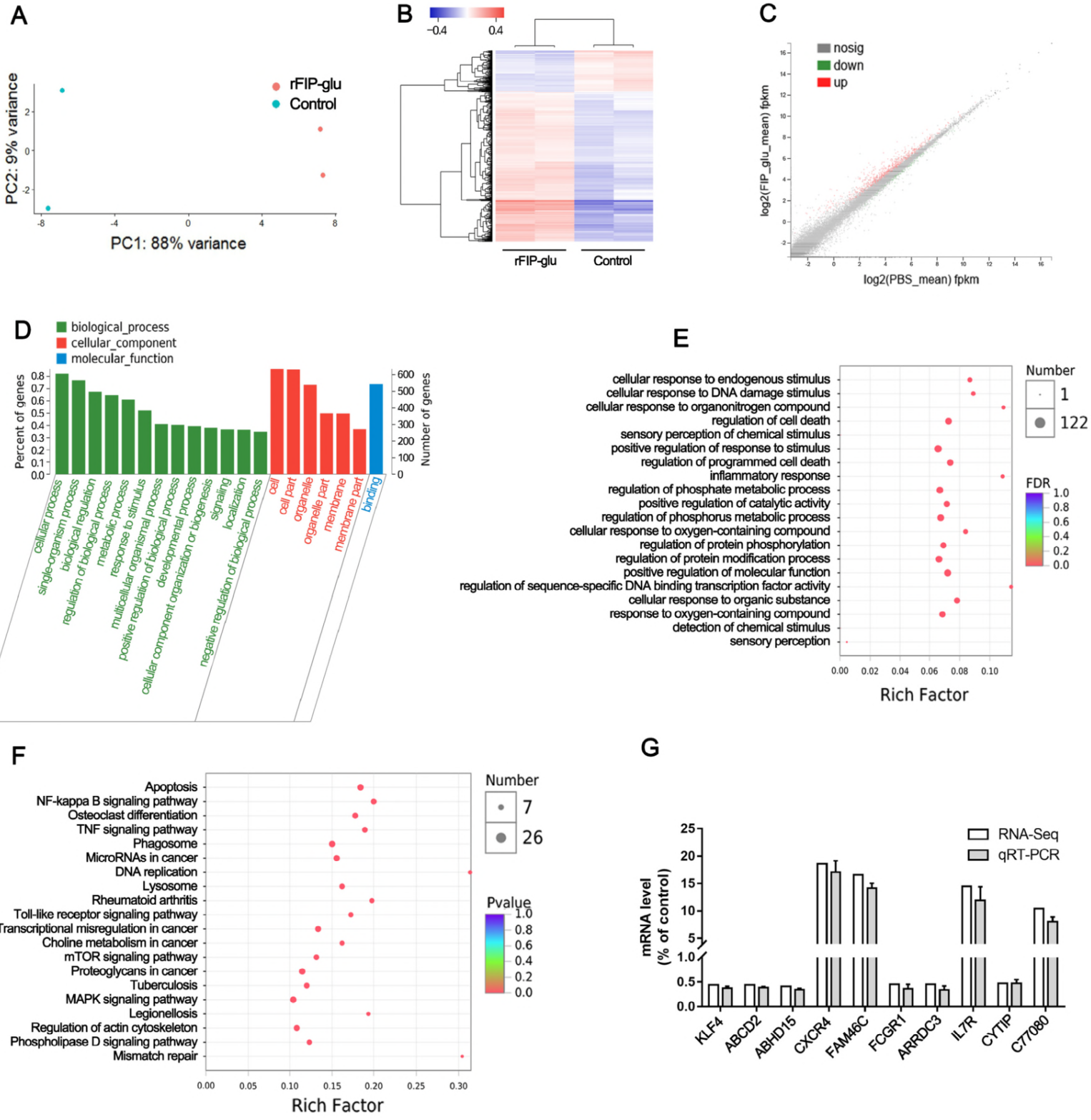
A
rFIP-glu
Control
PC2: 9% variance
PC1: 88% variance
B
−0.4
0.4
rFIP-glu
Control
C
nosig
down
up
log2(FIP_glu_mean) fpkm
log2(PBS_mean) fpkm
D
biological_process
cellular_component
molecular_function
Percent of genes
Number of genes
cellular process
single-organism process
biological regulation
regulation of biological process
metabolic process
response to stimulus
multicellular organismal process
positive regulation of biological process
developmental process
cellular component organization or biogenesis
signaling
localization
negative regulation of biological process
cell
cell part
organelle
organelle part
membrane
membrane part
binding
E
cellular response to endogenous stimulus
cellular response to DNA damage stimulus
cellular response to organonitrogen compound
regulation of cell death
sensory perception of chemical stimulus
positive regulation of response to stimulus
regulation of programmed cell death
inflammatory response
regulation of phosphate metabolic process
positive regulation of catalytic activity
regulation of phosphorus metabolic process
cellular response to oxygen-containing compound
regulation of protein phosphorylation
regulation of protein modification process
positive regulation of molecular function
regulation of sequence-specific DNA binding transcription factor activity
cellular response to organic substance
response to oxygen-containing compound
detection of chemical stimulus
sensory perception
Number
1
122
FDR
Rich Factor
F
Apoptosis
NF-kappa B signaling pathway
Osteoclast differentiation
TNF signaling pathway
Phagosome
MicroRNAs in cancer
DNA replication
Lysosome
Rheumatoid arthritis
Toll-like receptor signaling pathway
Transcriptional misregulation in cancer
Choline metabolism in cancer
mTOR signaling pathway
Proteoglycans in cancer
Tuberculosis
MAPK signaling pathway
Legionellosis
Regulation of actin cytoskeleton
Phospholipase D signaling pathway
Mismatch repair
Number
7
26
Pvalue
Rich Factor
G
RNA-Seq
qRT-PCR
mRNA level
(% of control)
KLF4
ABCD2
ABHD15
CXCR4
FAM46C
FCGR1
ARRDC3
IL7R
CYTIP
C77080

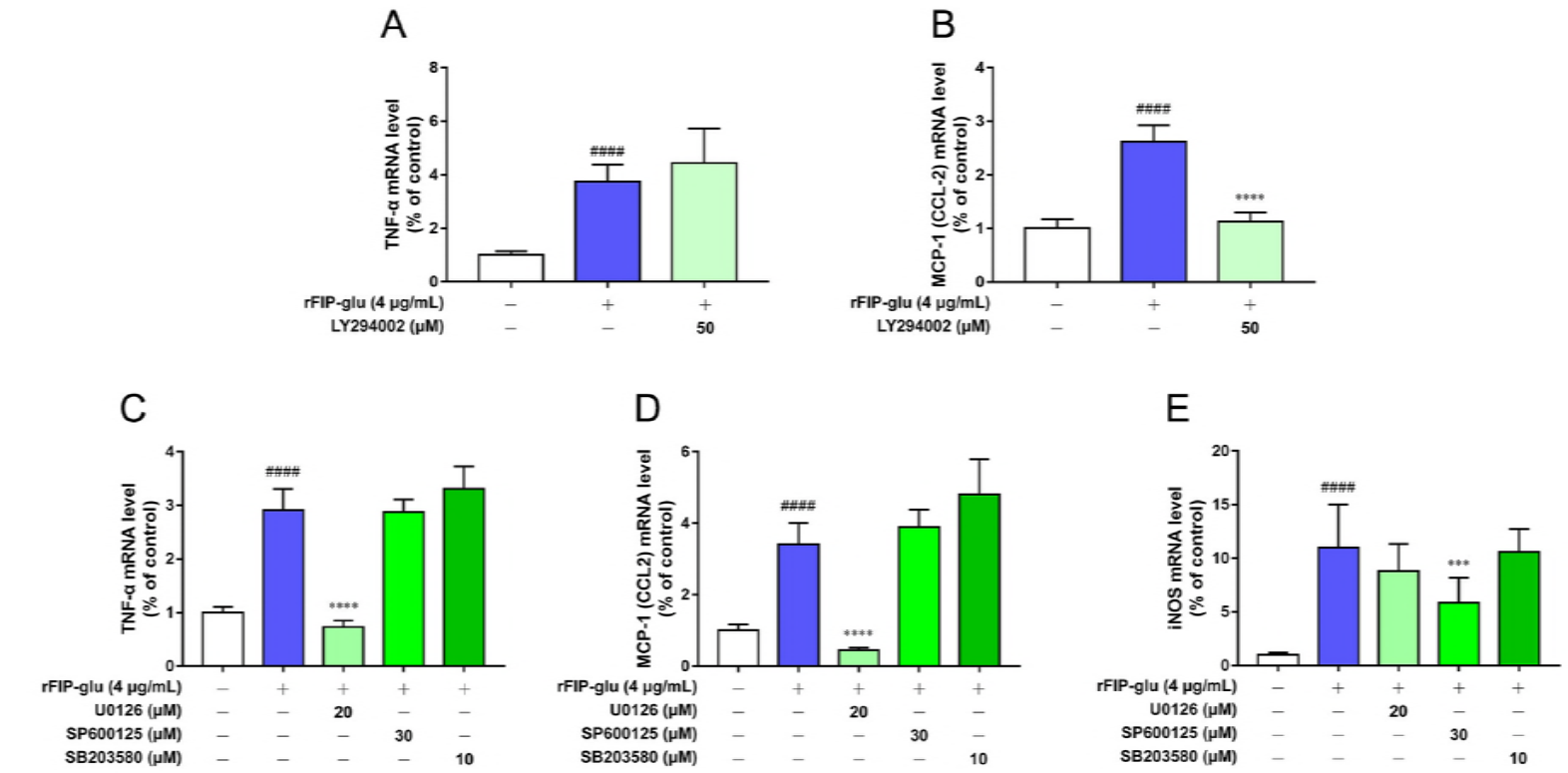
A
TNF-α mRNA level (% of control)
####
rFIP-glu (4 μg/mL) – + +
LY294002 (μM) – – 50
B
MCP-1 (CCL-2) mRNA level (% of control)
####
****
rFIP-glu (4 μg/mL) – + +
LY294002 (μM) – – 50
C
TNF-α mRNA level (% of control)
####
****
rFIP-glu (4 μg/mL) – + + + +
U0126 (μM) – – 20 – –
SP600125 (μM) – – – 30 –
SB203580 (μM) – – – – 10
D
MCP-1 (CCL2) mRNA level (% of control)
####
****
rFIP-glu (4 μg/mL) – + + + +
U0126 (μM) – – 20 – –
SP600125 (μM) – – – 30 –
SB203580 (μM) – – – – 10
E
iNOS mRNA level (% of control)
####
***
rFIP-glu (4 μg/mL) – + + + +
U0126 (μM) – – 20 – –
SP600125 (μM) – – – 30 –
SB203580 (μM) – – – – 10

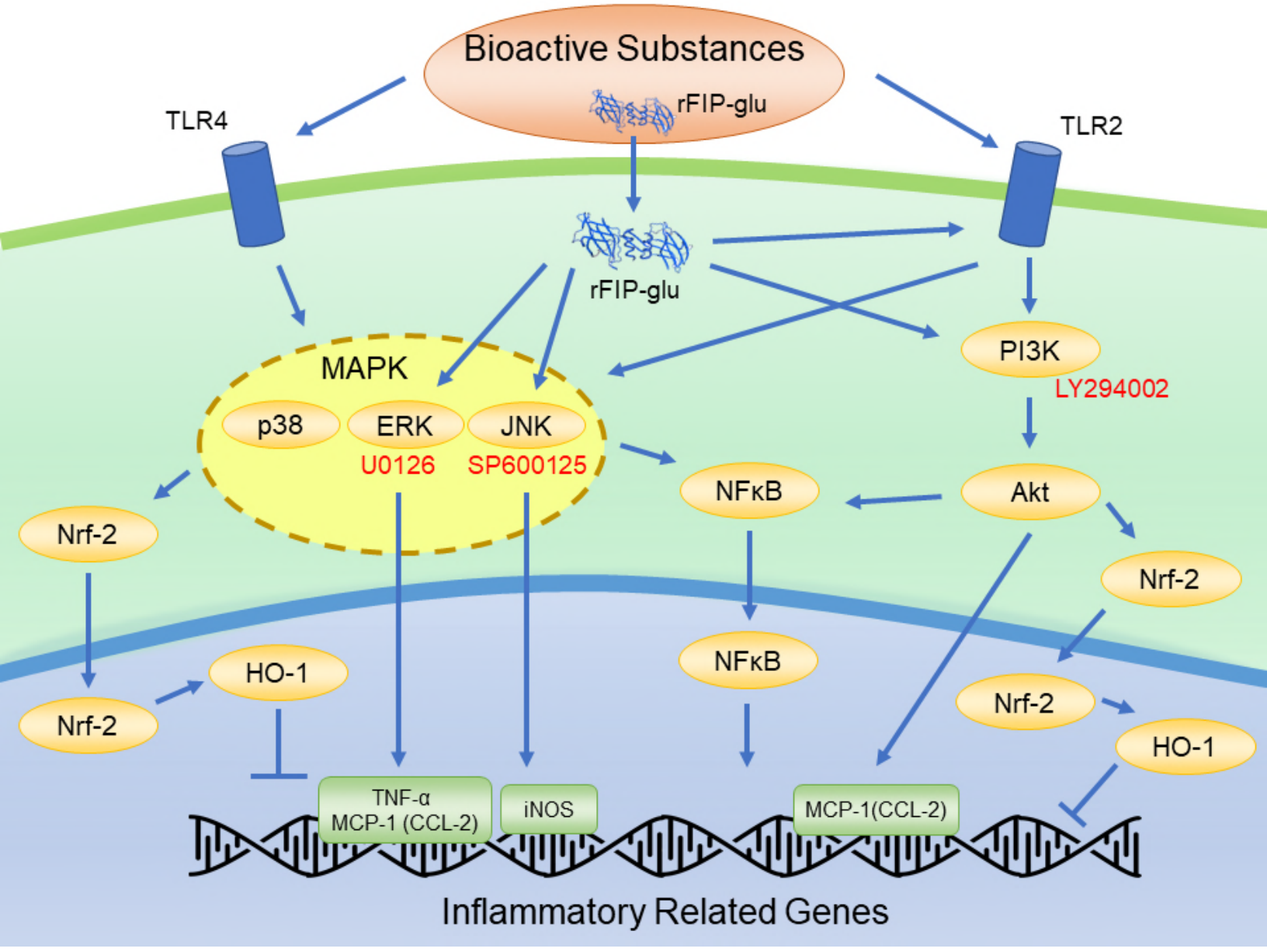
Bioactive Substances
rFIP-glu
TLR4
TLR2
rFIP-glu
MAPK
p38
ERK
JNK
U0126
SP600125
PI3K
LY294002
Akt
NFκB
Nrf-2
Nrf-2
HO-1
Nrf-2
NFκB
Nrf-2
HO-1
TNF-α
MCP-1 (CCL-2)
iNOS
MCP-1(CCL-2)
Inflammatory Related Genes